EUR 367.e

EUROPEAN ATOMIC ENERGY COMMUNITY - EURATOM

REFLECTION AND TRANSMISSION OF NEUTRONS BY THE MULTIPLE COLLISION METHOD

by

T. ASAOKA

1963

Joint Nuclear Research Center
Ispra Establishment - Italy

Reactor Physics Department
Applied Mathematical Physics Service

LEGAL NOTICE

This document was prepared under the sponsorship of the Commission of the European Atomic Energy Community (EURATOM).

Neither the EURATOM Commission, its contractors nor any person acting on their behalf :

1° — Make any warranty or representation, express or implied, with respect to the accuracy, completeness, or usefulness of the information contained in this document, or that the use of any information, apparatus, method, or process disclosed in this document may not infringe privately owned rights ; or

2° — Assume any liability with respect to the use of, or for damages resulting from the use of any information, apparatus, method or process disclosed in this document.

This report can be obtained, at the price of Belgian Francs 100, from : PRESSES ACADEMIQUES EUROPEENNES — 98, Chaussée de Charleroi, Brussels 6.

Please remit payments :

— to BANQUE DE LA SOCIETE GENERALE (Agence Ma Campagne) — Brussels — account No 964.558,

— to BELGIAN AMERICAN BANK AND TRUST COMPANY — New York — account No 121.86,

— to LLOYDS BANK (Foreign) Ltd. — 10 Moorgate - London E.C.2,

giving the reference : « EUR 367 . e — Reflection and transmission of neutrons by the multiple collision method »

This document was duplicated on the basis of the best available copy.

Printed by IMPRIMERIE L. VANMELLE, S.A., GHENT
Brussels, July 1963.

E U R 3 6 7 . e

REFLECTION AND TRANSMISSION OF NEUTRONS
BY THE MULTIPLE COLLISION METHOD
by T. ASAOKA

European Atomic Energy Community — EURATOM
Joint Nuclear Research Center
Ispra Establishment — Italy
Reactor Physics Department
Applied Mathematical Physics Service
Brussels, July 1963 — pages 67 — figures 31

The reflection and the transmission of neutrons for a homogeneous slab have been dealt with analytically by the multiple collision method or the random walk approach, where the elementary processes of the neutron are followed statistically in order of its spatial movement.

E U R 3 6 7 . e

REFLECTION AND TRANSMISSION OF NEUTRONS
BY THE MULTIPLE COLLISION METHOD
by T. ASAOKA

European Atomic Energy Community — EURATOM
Joint Nuclear Research Center
Ispra Establishment — Italy
Reactor Physics Department
Applied Mathematical Physics Service
Brussels, July 1963 — pages 67 — figures 31

The reflection and the transmission of neutrons for a homogeneous slab have been dealt with analytically by the multiple collision method or the random walk approach, where the elementary processes of the neutron are followed statistically in order of its spatial movement.

Under the assumption that the scattering of neutrons is spherically symmetric in the L system, the number of neutrons leaking from the slab with μ, a directional cosine of the emission angle, as a result of the N-th collision of an incident neutron has been derived. And further, the total number of the leakage neutrons, the total neutron current at the boundary of the slab and so on have been also written in the forms of an infinite series of the spherical Bessel functions.

The numerical results have been obtained by truncating the sum at the first five terms and it has been shown, by comparing some results with the exact ones, that the present approximation gives a very accurate result.

Moreover, the critical condition of the slab in the one-group approximation has been derived and shown that it exactly coincides with the one obtained in the previous work.

Under the assumption that the scattering of neutrons is spherically symmetric in the L system, the number of neutrons leaking from the slab with μ, a directional cosine of the emission angle, as a result of the N-th collision of an incident neutron has been derived. And further, the total number of the leakage neutrons, the total neutron current at the boundary of the slab and so on have been also written in the forms of an infinite series of the spherical Bessel functions.

The numerical results have been obtained by truncating the sum at the first five terms and it has been shown, by comparing some results with the exact ones, that the present approximation gives a very accurate result.

Moreover, the critical condition of the slab in the one-group approximation has been derived and shown that it exactly coincides with the one obtained in the previous work.

EUR 367.e

EUROPEAN ATOMIC ENERGY COMMUNITY - EURATOM

REFLECTION AND TRANSMISSION OF NEUTRONS BY THE MULTIPLE COLLISION METHOD

by

T. ASAOKA

1963

Joint Nuclear Research Center
Ispra Establishment - Italy

Reactor Physics Department
Applied Mathematical Physics Service

CONTENTS

KEY TO THE TABLES

KEY TO THE FIGURES

Fig. 1 A typical path of the incident neutron in the slab

Fig. 2 Flow diagram of calculations in the constant cross section approximation

Fig. 3 Number of neutrons reflected after the first collision (monodirectional source)

Fig. 4 Number of neutrons reflected after the second collision (monodirectional source)

Fig. 5 Number of neutrons reflected after the third collision (monodirectional source)

Fig. 6 Number of neutrons reflected after the 5-th collision (monodirectional source)

Fig. 7 Number of neutrons reflected after the 7-th collision (monodirectional source)

Fig. 8 Number of neutrons reflected after the 10-th collision (monodirectional source)

Fig. 9 Number of neutrons reflected after the 15-th collision (monodirectional source)

Fig. 10 Number of neutrons reflected after the 20-th collision (monodirectional source)

Fig. 11 Number of neutrons reflected after the 30-th collision (monodirectional source)

Fig. 12 Number of neutrons reflected after the 50-th or the 70-th collision (monodirectional source)

Fig. 13 Number of neutrons reflected by the slab with $\Sigma_a =$ 2 or 4 after the N-th collision (monodirectional source)

Fig. 14 Number of neutrons transmitting after the first collision (monodirectional source)

Fig. 15 Number of neutrons transmitting after the second collision (monodirectional source)

Fig. 16 Number of neutrons transmitting after the third collision (monodirectional source)

Fig. 17 Number of neutrons transmitting after the 5-th collision (monodirectional source)

Fig. 18 Number of neutrons transmitting after the 7-th collision (monodirectional source)

REFLECTION AND TRANSMISSION OF NEUTRONS BY THE MULTIPLE COLLISION METHOD

SUMMARY

The reflection and the transmission of neutrons for a homogeneous slab have been dealt with analytically by the multiple collision method or the random walk approach, where the elementary processes of the neutron are followed statistically in order of its spatial movement.

Under the assumption that the scattering of neutrons is spherically symmetric in the L system, the number of neutrons leaking from the slab with μ, a directional cosine of the emission angle, as a result of the N-th collision of an incident neutron has been derived. And further, the total number of the leakage neutrons, the total neutron current at the boundary of the slab and so on have been also written in the forms of an infinite series of the spherical Bessel functions.

The numerical results have been obtained by truncating the sum at the first five terms and it has been shown, by comparing some results with the exact ones, that the present approximation gives a very accurate result.

Moreover, the critical condition of the slab in the one-group approximation has been derived and shown that it exactly coincides with the one obtained in the previous work.

1. Introduction

The multiple collision method is a new analytical method for dealing with neutron transport problems. This method is based on a viewpoint different from that of the Boltzmann equation, that is, the life-cycle viewpoint in contrast to the neutron-balance one.

The one-group critical condition has already been derived accurately by this method, for a homogeneous slab in which scattering is spherically symmetric in the L system (Asaoka, 1961). The two-group critical condition for the same system has been also derived according to this technique (Asaoka and Nakahara, 1962). In these previous works, the elementary processes of the neutron were followed statistically in order of time and then the critical condition was obtained from the convergence of the total number of neutrons in the system as time proceeds indefinitely.

The present report is concerned with a further development of the multiple collision method for treating the reflection and the transmission of neutrons for a homogeneous slab. Here, the elementary processes are followed statistically in order of the spatial movement of the neutron.

Although a number of investigations have been made on the problem regarding to the reflection or the transmission of radiation (for example, Grosjean, 1958), it seems that their methods are not sufficient to briefly obtain the accurate and plentiful information. In this report, it will be shown that the problem can be treated efficiently by the multiple collision method.

2. Formulations

Consideration will be given to the case of an infinite homogeneous slab with finite thickness a in which the neutrons are scattered in spherical symmetry in the L system, on the basis of the constant cross section approximation. To the case that the cross section for the medium is assumed according to the two-group model, the method is easily extended as shown later.

Let x be the space coordinate, μ the directional cosine of the neutron velocity, Σ the macroscopic total cross section and c the mean number of secondaries per collision.

Now, consider one incident neutron with a directional cosine $\mu=\mu_1$, upon a surface of the slab, $x = 0$. It will travel for a certain distance r_1, in the direction with $\mu=\mu_1$, before it collides with a nucleus. Since this probability is $\exp(-\Sigma r_1)$ and the collision probability in dr_1 at r_1 is Σdr_1, the fractional number of neutrons with directional cosines between μ_2 and $\mu_2+d\mu_2$ as a result of this collision will be $(c\Sigma/2)\exp(-\Sigma r_1)dr_1 d\mu_2$. They will then travel for a certain distance r_2 in the direction μ_2 until they meet another nuclei. As a result of this second collision, the fractional number of neutrons between μ_3 and $\mu_3+d\mu_3$ will amount to $(c\Sigma/2)^2\exp[-\Sigma(r_1+r_2)]dr_1 dr_2 d\mu_2 d\mu_3$. This process of movement will continue until the neutron leaks out of the slab after the N-th collision as shown in Fig. 1.

Thus the fractional number of neutrons leaking from the slab with directional cosines between μ and $\mu+d\mu$ as a result of the N-th collision after following a typical path shown in Fig. 1, is given by

$$(c\Sigma/2)^N \exp[-\Sigma(r_1+r_2+\cdots+r_N+r)]dr_1\cdots dr_N\, d\mu_2\cdots d\mu_N d\mu, \quad N\geq 1. \tag{1}$$

Before performing integrations over all allowable paths to obtain the number of neutrons reflected by or transmitting the slab, we must take into account some restrictions imposed upon the range of integration variables in order to exclude the neutrons which have left the slab after the $(j-1)$-th collision. These are written as follows:

$$0 < \sum_{k=1}^{j} \gamma_k \mu_k < a \,, \quad j = 1, 2, \cdots, N. \tag{2}$$

Besides this, an another condition must be imposed in order to make the neutrons leave the slab with a directional cosine μ after the N-th collision:

$$\sum_{j=1}^{N} \gamma_j \mu_j + \gamma \mu = \gamma_0 = \begin{cases} 0, & \text{for the reflection,} \\ a, & \text{for the transmission,} \end{cases} \quad N \geq 1. \tag{3}$$

This condition (3) can be rewritten in a form of Fourier representation of the Dirac delta function:

$$\begin{aligned} \delta\left(\gamma - \frac{\gamma_0}{\mu} + \frac{1}{\mu}\sum_{j=1}^{N} \gamma_j \mu_j\right) &= \mp \frac{\mu}{2\pi} \int_{-\infty}^{\infty} d\rho \exp\left[i\rho\left(\mu\gamma - \gamma_0 + \sum_{j=1}^{N} \gamma_j \mu_j\right)\right] \\ &= \mp \frac{\mu}{\pi a} \int_{-\infty}^{\infty} d\gamma_{N+1} \exp\left[\frac{2i}{a}\gamma_{N+1}\left(\mu\gamma - \gamma_0 + \sum_{j=1}^{N} \gamma_j \mu_j\right)\right], \end{aligned} \tag{4}$$

where the upper sign is applied to the case of reflection $(\mu < 0)$ and the lower one to the case of transmission $(\mu > 0)$. The conditions (2) can be taken into account through Dirichlet's discontinuity factors:

$$\frac{1}{\pi} \int_{-\infty}^{\infty} d\gamma_j \frac{\sin \gamma_j}{\gamma_j} e^{i\gamma_j z_j} = \begin{cases} 1, & \text{when } |z_j| < 1, \\ 0, & \text{when } |z_j| > 1, \end{cases} \quad j = 1, 2, \cdots, N.$$

Then introducing the N discontinuity factors and the Fourier representation of the δ function, the number of neutrons reflected by or transmitting the slab in a direction with μ as a result of the N-th collision of one incident neutron with $\mu=\mu_1$, is written as follows:

$$\eta_N(\chi_0,\mu;\mu_1)=\mp\frac{\mu}{\pi a}\left(\frac{c\Sigma}{2}\right)^N\int_0^\infty d\gamma_1\cdots d\gamma_N d\gamma\int_{-1}^{1}d\mu_2\cdots d\mu_N$$
$$\times\prod_{j=1}^{N}\left\{\frac{1}{\pi}\int_{-\infty}^{\infty}d\chi_j\, j_0(\chi_j)\exp\left[i\chi_j\left(\frac{2}{a}\sum_{k=1}^{j}\gamma_k\mu_k-1\right)\right]\right\}\int_{-\infty}^{\infty}d\chi_{N+1}\exp\left[\frac{2i}{a}\chi_{N+1}\left(\mu\gamma-\chi_0+\sum_{j=1}^{N}\gamma_j\mu_j\right)\right]e^{-\Sigma(\gamma_1+\cdots+\gamma_N+\gamma)}, \tag{5}$$

where $j_n(\chi)$ is the spherical Bessel function. Replacing χ_j by $y_j=(2/(\Sigma a))\sum_{k=j}^{N+1}\chi_k$ $(j=1,\cdots,N+1)$ and performing the integrations over μ_j $(j=2,\cdots,N)$, γ_j $(j=1,\cdots,N)$ and γ, Eq. (5) is reduced to

$$\eta_N(\chi_0,\mu;\mu_1)=\mp\frac{\mu}{2\pi}\int_{-\infty}^{\infty}dy\,\frac{\exp[-i\Sigma y(\chi_0-a/2)]}{1-i\mu y}G_{N+1}(y;\mu_1), \tag{6}$$

in which the independent variable y_{N+1} is replaced by y. The functions $G_{j+1}(y;\mu_1)$'s satisfy the following recurrence relation:

$$\left.\begin{aligned}
G_{j+1}(y;\mu_1)&=\frac{c\Sigma a}{2\pi}\int_{-\infty}^{\infty}d\chi\, j_0\left[\frac{\Sigma a}{2}(\chi-y)\right]\frac{\tan^{-1}\chi}{\chi}G_j(\chi;\mu_1),\quad j=N,N-1,\cdots,2,\\
G_2(y;\mu_1)&=\frac{c\Sigma a}{4\pi}\int_{-\infty}^{\infty}d\chi\, j_0\left[\frac{\Sigma a}{2}(\chi-y)\right]\frac{\exp\left(-i\frac{\Sigma a}{2}\chi\right)}{1-i\mu_1\chi}\\
&=\frac{c/2}{1-i\mu_1 y}\left[\exp\left(-i\frac{\Sigma a}{2}y\right)-\exp\left(i\frac{\Sigma a}{2}y\right)\exp\left(-\frac{\Sigma a}{\mu_1}\right)\right].
\end{aligned}\right\} \tag{7}$$

Now it is convenient to expand $G_{j+1}(y;\mu_1)$'s in the spherical Bessel functions:

$$G_{j+1}(y;\mu_1)=\sum_{m=0}^{\infty}b_m^{j+1}(\mu_1)j_m\left(\frac{\Sigma a}{2}y\right),\quad j=N,N-1,\cdots,1. \tag{8}$$

Then by using the Gegenbauer's addition theorem:

$$j_0(x-y)=\sum_{n=0}^{\infty}(2n+1)j_n(x)j_n(y)$$

and the orthogonality relation for the spherical Bessel functions, the recurrence relation (7) is rewritten as follows:

$$\left.\begin{aligned}&\frac{1}{(2l+1)C}f_n^{l+1}(\mu_1)=\sum_{\substack{m=0\\ n+m=\text{even}}}^{\infty}f_m^{l}(\mu_1)J(n,m)\,,\quad l=N,N-1,\cdots,2,\\&f_n^{2}(\mu_1)=(2n+1)\frac{c\Sigma a}{2\mu_1}j_n\left(-i\frac{\Sigma a}{2\mu_1}\right)\exp\left(-\frac{\Sigma a}{2\mu_1}\right),\end{aligned}\right\}\qquad(9)$$

where

$$J(n,m)=\frac{2\alpha}{\pi}\int_0^{\infty}dy\,j_n(\alpha y)j_m(\alpha y)\frac{\tan^{-1}y}{y}\,,\quad \alpha=\frac{\Sigma a}{2}\,.\qquad(10)$$

Upon substituting Eq. (8) into Eq. (6), we get

$$n_N(x_0,\mu;\mu_1)=\exp\left(-\frac{\Sigma a}{2|\mu|}\right)\sum_{m=0}^{\infty}f_m^{N+1}(\mu_1)j_m\left(-i\frac{\Sigma a}{2\mu}\right)\,,\qquad(11)$$

of which the coefficients $f_m^{N+1}(\mu_1)$ are to be determined by the recurrence relation (9).

The total number of neutrons reflected by or transmitting the slab in a direction with μ as a result of the incidence of one neutron with $\mu=\mu_1$, is given by

$$n(x_0,\mu;\mu_1)=\sum_{N=1}^{\infty}n_N(x_0,\mu;\mu_1)+\delta(\mu-\mu_1)\exp(-\Sigma a/\mu_1)\,.\qquad(12)$$

The infinite sum in this equation is written in the following form according to Eq. (11):

$$\sum_{N=1}^{\infty} \eta_N(\tau_0,\mu;\mu_1) = \exp\left(-\frac{\Sigma a}{2|\mu|}\right)\sum_{m=0}^{\infty} f_m(\mu_1) j_m\left(-i\frac{\Sigma a}{2\mu}\right), \tag{13}$$

where $f_m(\mu_1)=\sum_{N=1}^{\infty} f_m^{N+1}(\mu_1)$ is to be determined by an infinite set of linear equations which are derived from Eq. (9):

$$\frac{1}{(2m+1)c} f_m(\mu_1) = \frac{1}{(2m+1)c} f_m^2(\mu_1) + \sum_{\substack{n=0 \\ m+n=\text{even}}}^{\infty} f_n(\mu_1) J(m,n), \tag{14}$$

$$m=0,1,2,\cdots .$$

The total number of neutrons reflected by or transmitting the slab as a result of the incidence of one neutron with $\mu=\mu_1$ is obtained in the following form by integration of Eq. (12) with respect to μ from -1 to zero of from zero to 1:

$$\eta(\tau_0;\mu_1) = \sum_{m=0}^{\infty} f_m(\mu_1)\int_1^{\infty}\frac{dt}{t^2}\exp\left(-\frac{\Sigma a}{2}t\right) j_m\left(\pm i\frac{\Sigma a}{2}t\right) + \Delta \exp\left(-\frac{\Sigma a}{\mu_1}\right), \tag{15}$$

where

$$\Delta = \begin{cases} 0, & \text{for the reflection,} \\ 1, & \text{for the transmission.} \end{cases}$$

When the integration with respect to μ is performed after multiplying $\eta(\tau_0,\mu;\mu_1)$ by $\mp\mu$, the total neutron current in the direction of the outward normal to the surface of the slab is obtained:

$$J(\tau_0;\mu_1) = \sum_{m=0}^{\infty} f_m(\mu_1)\int_1^{\infty}\frac{dt}{t^3}\exp\left(-\frac{\Sigma a}{2}t\right) j_{2n}\left(\pm i\frac{\Sigma a}{2}t\right) + \Delta\mu_1 \exp\left(-\frac{\Sigma a}{\mu_1}\right), \tag{16}$$

Then the so-called albedo for this slab for the case of the incidence of neutrons with $\mu=\mu_1$ can be obtained by

$$A(\mu_1)=J(0;\mu_1)/\mu_1 \ . \tag{17}$$

In case of that the angular distribution of incident neutrons is spherically symmetric, that is, the number of incident neutrons with directional cosines between μ_1 and $\mu_1+d\mu_1$ is $d\mu_1$ when the total number is normalized to unity, Eqs. (11)$\sim$(13) and (15)$\sim$(17) are modified as follows:

$$n_N(\tau_0,\mu)=\exp\left(-\frac{\Sigma a}{2|\mu|}\right)\sum_{m=0}^{\infty} f_m^{N+1} j_m\left(-i\frac{\Sigma a}{2\mu}\right), \tag{11'}$$

$$n(\tau_0,\mu)=\sum_{N=1}^{\infty} n_N(\tau_0,\mu)+\Delta\exp(-\Sigma a/\mu), \tag{12'}$$

$$\sum_{N=1}^{\infty} n_N(\tau_0,\mu)=\exp\left(-\frac{\Sigma a}{2|\mu|}\right)\sum_{m=0}^{\infty} f_m j_m\left(-i\frac{\Sigma a}{2\mu}\right), \tag{13'}$$

$$n(\tau_0)=\sum_{m=0}^{\infty} f_m\int_1^{\infty}\frac{dt}{t^2}\exp\left(-\frac{\Sigma a}{2}t\right)j_m\left(\pm i\frac{\Sigma a}{2}t\right)+\Delta E_2(\Sigma a), \tag{15'}$$

$$J(\tau_0)=\sum_{m=0}^{\infty} f_m\int_1^{\infty}\frac{dt}{t^3}\exp\left(-\frac{\Sigma a}{2}t\right)j_m\left(\pm i\frac{\Sigma a}{2}t\right)+\Delta E_3(\Sigma a), \tag{16'}$$

$$A=2J(0). \tag{17'}$$

The coefficients f_m^{N+1} and $f_m=\sum_{N=1}^{\infty} f_m^{N+1}$ are determined by the following recurrence relation (9') and the set of simultaneous equations (14'), respectively:

$$\left.\begin{aligned}&\frac{1}{(2n+1)c}f_n^{j+1}=\sum_{\substack{m=0\\ n+m=\text{even}}}^{\infty} f_m^{j}J(n,m), \quad j=N,N-1,\cdots,2,\\ &f_n^{2}=(2n+1)\frac{c\Sigma a}{2}\int_1^{\infty}\frac{dt}{t}\exp\left(-\frac{\Sigma a}{2}t\right)j_n\left(-i\frac{\Sigma a}{2}t\right),\end{aligned}\right\} \tag{9'}$$

$$\frac{1}{(2m+1)c}f_m=\frac{1}{(2m+1)c}f_m^{2}+\sum_{\substack{n=0\\ m+n=\text{even}}}^{\infty} f_n J(m,n), \quad m=0,1,2,\cdots. \tag{14'}$$

A comment will be inserted here, on the critical condition of the slab in the one-group approximation. Also to the case of that there are fissionable nuclei in the medium, the equations having been derived can be applied, if discussions are restricted to monochromatic neutrons. Therefore, in case of that $c>1$, the total number of neutrons leaking from the slab must diverge beyond all bounds at the critical thickness. In other words, the critical condition in the one-group approximation must be derived from the divergence of

$$n(0;\mu_1)+n(a;\mu_1),\ J(0;\mu_1)+J(a;\mu_1),\ n(0)+n(a) \quad \text{or} \quad J(0)+J(a).$$

Since these are given in the following form as seen from Eqs. (15), (16), (15') and (16'):

$$\sum_{m=0}^{\infty} B_{2m} f_{2m}(\mu_1)+C \quad \text{or} \quad \sum_{m=0}^{\infty} B_{2m} f_{2m}+C',$$

where B_{2m} , C and C' are bounded functions of Σa , the critical condition should be given by the condition of divergence of $f_{2m}(\mu_1)$ and f_{2m} . This condition is that the determinant of coefficients for $f_{2m}(\mu_1)$'s or f_{2m} 's in Eq.(14) or (14') vanishes; that is,

$$\left| \frac{\delta_{2n,2m}}{(4m+1)C} - J(2n,2m) \right| = 0, \quad n,m=0,1,2,\cdots . \tag{18}$$

This condition (18) is nothing but the one-group critical condition that was derived in the previous work by the author (Asaoka, 1961).

Now we shall consider the reflection and the transmission of neutrons in case of that the cross section for the medium is assumed according to the two-group model. Let Σ_1 and Σ_2 be the macroscopic total cross section for the fast group and the thermal group, respectively, and c_1 and c_2 the mean number of secondaries per collision for each group. And further, let assume that N_c is the number of collisions required to decrease the energy of the incident neutrons to the thermal value.

Following the same procedures as those in the constant cross section approximation, the number of thermal neutrons reflected by or transmitting the slab with μ as a result of the N-th collision of one incident neutron with $\mu=\mu_1$ is written as

$$n_N^{th}(x_0,\mu;\mu_1) = \mp\frac{\mu}{2\pi}\int_{-\infty}^{\infty} dy\, \frac{\exp[-i\Sigma_2 y(x_0-a/2)]}{1-i\mu y} G_{N+1}(y;\mu_1), \qquad N\geq N_c\geq 1, \tag{19}$$

where

$$\left.\begin{aligned} G_{j+1}(y;\mu_1) &= \frac{c_2\Sigma_2 a}{2\pi}\int_{-\infty}^{\infty} dx\, j_0\left[\frac{\Sigma_2 a}{2}(x-y)\right]\frac{\tan^{-1}x}{x} G_j(x;\mu_1), \qquad j=N, N-1, \cdots, N_c+1,\\ G_{j+1}\left(\frac{\Sigma_1}{\Sigma_2}y;\mu_1\right) &= \frac{c_1\Sigma_1 a}{2\pi}\int_{-\infty}^{\infty} dx\, j_0\left[\frac{\Sigma_2 a}{2}(x-y)\right]\frac{\tan^{-1}x}{x} G_j\left(\frac{\Sigma_1}{\Sigma_2}x;\mu_1\right), \qquad j=N_c, \cdots, 2,\\ G_2\left(\frac{\Sigma_1}{\Sigma_2}y;\mu_1\right) &= \frac{c_1\Sigma_1 a}{4\pi}\int_{-\infty}^{\infty} dx\, j_0\left[\frac{\Sigma_1 a}{2}(x-y)\right]\frac{\exp(-i\frac{\Sigma_1 a}{2}x)}{1-i\mu_1 x}. \end{aligned}\right\} \tag{20}$$

Thus the total number of thermal neutrons leaking from the slab with μ is given by

$$\begin{aligned} n_{th}(x_0,\mu;\mu_1) &= \sum_{N=N_c}^{\infty} n_N^{th}(x_0,\mu;\mu_1)\\ &= \mp\frac{\mu}{2\pi}\int_{-\infty}^{\infty} dy\, \frac{\exp[-i\Sigma_2 y(x_0-a/2)]}{1-i\mu y}\sum_{N=N_c}^{\infty} G_{N+1}(y;\mu_1), \end{aligned} \tag{21}$$

where

$$\sum_{N=N_c}^{\infty} G_{N+1}(y;\mu_1) = G_{N_c+1}(y;\mu_1) + \frac{c_2\Sigma_2 a}{2\pi}\int_{-\infty}^{\infty} dx\, j_0\left[\frac{\Sigma_2 a}{2}(x-y)\right]\frac{\tan^{-1}x}{x}\sum_{N=N_c+1}^{\infty} G_N(x;\mu_1), \qquad (22)$$

as easily seen from the first equation in Eq. (20).
Here the functions $G_{j+1}(y;\mu_1)$'s are expanded in the spherical Bessel functions:

$$\left.\begin{aligned} &\sum_{N=N_c}^{\infty} G_{N+1}(y;\mu_1) = \sum_{m=0}^{\infty} f_m'(\mu_1) j_m\left(\frac{\Sigma_2 a}{2} y\right), \\ &G_{j+1}\left(\frac{\Sigma_1}{\Sigma_2} y;\mu_1\right) = \sum_{m=0}^{\infty} f_m^{j+1}(\mu_1) j_m\left(\frac{\Sigma_1 a}{2} y\right), \quad j = N_c, N_c-1, \cdots, 1, \end{aligned}\right\} \qquad (23)$$

of which the coefficients are to be determined by the following equations:

$$\left.\begin{aligned} &\frac{1}{(2m+1)c_2} f_m'(\mu_1) = \frac{1}{(2m+1)c_2} f_m^{N_c+1}(\mu_1) + \sum_{\substack{n=0 \\ m+n=\text{even}}}^{\infty} f_n'(\mu_1) J_2(m,n), \\ &\frac{1}{(2m+1)c_1} f_m^{j+1}(\mu_1) = \sum_{\substack{n=0 \\ m+n=\text{even}}}^{\infty} f_m^{j}(\mu_1) J_1(m,n), \quad j = N_c, N_c-1, \cdots, 2, \\ &f_m^{2}(\mu_1) = (2m+1)\frac{c_1\Sigma_1 a}{2\mu_1} j_m\left(-i\frac{\Sigma_1 a}{2\mu_1}\right)\exp\left(-\frac{\Sigma_1 a}{2\mu_1}\right), \end{aligned}\right\} \qquad (24)$$

where $J_2(m,n)$ and $J_1(m,n)$ are given by Eq. (10) in which $\alpha = \Sigma_2 a/2$ and $\Sigma_1 a/2$, respectively.
Thus, combining Eq. (21) with the first equation in Eq. (23), we get

$$n_{th}(x_0,\mu;\mu_1) = \exp\left(-\frac{\Sigma_2 a}{2|\mu|}\right)\sum_{m=0}^{\infty} f_m'(\mu_1) j_m\left(-i\frac{\Sigma_2 a}{2\mu}\right). \qquad (25)$$

Similarly, the number of thermal neutrons leaking out after the N-th collision, $\eta_N^{th}(\tau_0,\mu;\mu_1)$ shown in Eq. (19) can be easily written also in a form as that of Eq. (25), and further the total number of thermal neutrons leaking from the slab, $\eta_{th}(\tau_0;\mu_1)$, and so on can be obtained also easily, even for the case of the incidence of isotropic neutrons.

3. Numerical Results and Discussions

Since all expressions such as $\eta_N(\tau_0,\mu;\mu_1)$ in Eq. (11), $\eta_N(\tau_0,\mu)$ in Eq. (11') have been written in the form of an infinite sum, we are forced to truncate it at $m=M$ for obtaining the numerical results. We shall call this approximation as the j_M-approximation.

The flow diagram of calculations to get the numerical results in the constant cross section approximation is shown in Fig. 2. And the concrete expressions of the functions with $n\leq 4$ which are located at the starting points in the flow diagram, are shown in Appendix I.

In the j_M-approximation, the coefficients $f_n^{j+1}(\mu_1)$, $f_n(\mu_1)$, f_n^{j+1} and f_n are determined approximately by solving the equations obtained from Eqs. (9), (14), (9') and (14'), by retaining only $f_n^{j}(\mu_1)$, $f_n(\mu_1)$, f_n^{j} and f_n with $n\leq M$, respectively. As seen from Eqs. (14) and (14'), $f_{2n}(\mu_1)$'s and f_{2n} 's are coupled only with one another, and not with $f_{2n+1}(\mu_1)$'s and f_{2n+1} 's, respectively. Therefore, the expressions for these coefficients with an even suffix in the j_{2M+1} -approximation are the same as those in the j_{2M} -approximation and the ones with an odd suffix in the j_{2M} -approximation are the same as those in the j_{2M-1} -approximation. The expressions of $f_n(\mu_1)$'s up to in the j_4-approximation are shown in Appendix II. The expressions of f_n's are the same as these except that $f_n^2(\mu_1)$'s in the numerators are replaced by f_n^2 's.

Numerical computations are carried out for the slab with $C = 1$, for various values of the parameters shown in Table 1. The results for the three cases of the monodirectional source with $\mu_1 = 1$, 0.5 and 0.1, respectively, are shown in Figs. 3∼26 and in Tables 2 and 3.

The number of neutrons reflected by or transmitting the slab with μ after the N-th collision has been calculated in the j_4 - approximation. These results for $N = 1$ are compared with the exact ones which are obtained directly by performing the integration with respect to y after substituting $G_2(y;\mu_1)$ shown in Eq. (7) into Eq. (6). As seen from Figs. 3 and 14, the present approximation gives very accurate results for the case that the values of μ_1 are not close to zero, but it becomes to introduce some error to these results especially for the larger values of Σa when the values of μ_1 decrease close to zero. This error, however, may be reduced to be smaller as the value of N increases because the values of $f_4^{N+1}(\mu_1)$ become small compared with the ones of $f_0^{N+1}(\mu_1)$ (see Eq. (11)).

As seen from Figs. 3∼12, the values of $\eta_N(0,\mu;\mu_1)$ become to depend strongly on the value of Σa as N goes up to larger values, as expected, especially for the case of that $\mu_1 = 1$. And the curves are convex, that is, $\eta_N(0,\mu;\mu_1)$ gradually decreases around $|\mu| = 1$ as $|\mu|$ goes down to smaller values, for the smaller N, but they become to be concave as N becomes larger. This can be interpreted by taking into consideration that the positions at which the neutrons have suffered the final collision become to distribute uniformly within the slab.

The dependency of $\eta_N(0,\mu;\mu_1)$ on the value of μ_1 is as follows. For the smaller values of N, $\eta_N(0,\mu;\mu_1)$ increases as μ_1 decreases, as expected, especially for the smaller Σa. As the value of N becomes large, however, it turns to decrease as μ_1 does, especially for the larger Σa. This is understandable because $\eta_N(0,\mu;\mu_1)$ for large N comes mainly from the neutrons which have undergone the first collision near the center of the slab. Fig. 13 shows $\eta_N(0,\mu;\mu_1)$ for the slab with Σa = 2 and 4 as a function of N.

In Figs. 14 $\sim$ 24 are shown $\eta_N(a,\mu;\mu_1)$'s, the number of neutrons transmitting the slab with μ as a result of the N-th collision of one incident neutron with $\mu=\mu_1$. For the smaller values of N, on the whole, $\eta_N(a,\mu;\mu_1)$ for the smaller Σa is larger than that for the larger Σa, especially for small μ_1 and μ. But as the value of N increases, $\eta_N(a,\mu;\mu_1)$ for the smaller Σa becomes smaller than that for the larger Σa, especially for the large μ_1 and μ, because it depends upon the value of the probability that the neutrons take collisions N times within the slab, multiplied by the transmission probability. This may be clarified by comparing the curves for Σa = 2 with the ones for Σa = 4 shown in Fig. 24.

The curves of $\eta_N(a,\mu;\mu_1)$ are convex for the smaller Σa but they turn to be concave as the value of Σa increases, because the positions at which the neutrons have undergone the final collision may become to be far from the boundary of the slab. And further, it is seen that for the smaller Σa, the values of $\eta_N(a,\mu;\mu_1)$ depend strongly on the value of μ_1, and increase as μ_1 becomes small. Contrary to this, $\eta_N(a,\mu;\mu_1)$ for the larger Σa decreases as μ_1 does.

It may be worthwhile to mention that $\eta_N(a,\mu;\mu_1)$ becomes to have the same values as those of $\eta_N(0,\mu;\mu_1)$ as the value of N increases. This is a natural consequence because the spatial distribution of neutrons within the slab comes to be symmetric. The value of N from which both

the values of $\eta_N(a,\mu;\mu_1)$ and $\eta_N(0,\mu;\mu_1)$ nearly coincide with one another, in other words, the terms with odd m in the infinite sum in Eq. (11) can be neglected compared to ones with even m, is larger for the larger Σa, for example, these values for Σa = 0.5, 2 and 4 are about 10, 20 and 50, respectively.

Figure 25 or 26 shows the results of the total number of neutrons reflected by or transmitting the slab with μ, $\eta(0,\mu;\mu_1)$ or $\eta(a,\mu;\mu_1)$, in the f_4-approximation. Comparing Fig. 25 with Fig. 3, it is seen that the contribution of $\eta_1(0,\mu;\mu_1)$ amounts to more than half of the total number for the smaller Σa, but it decreases to ca. 20 % as the value of Σa becomes larger, especially for the case of that $\mu_1 = 1$. In the case of the transmission, the contribution of $\eta_1(a,\mu;\mu_1)$ to the total number of neutrons having transmitted the slab after suffering collisions once at least, amounts to ca. 50 % for Σa = 0.5 and decreases to several % for Σa = 4. Therefore, these results of the total number show that the values depend upon the ones of μ and μ_1 in a similar manner to those for $\eta_1(\tau_0,\mu;\mu_1)$ for the smaller Σa and to those for $\eta_N(\tau_0,\mu;\mu_1)$ with large N for the larger Σa.

The total number of neutrons reflected by or transmitting the slab, $\eta(0;\mu_1)$ or $\eta(a;\mu_1)$, is calculated in the f_1- and f_4-approximations. The results in the f_4-approximation are shown in Table 2. Since C = 1, that is, there is no absorption of neutrons, the sum of $\eta(0;\mu_1)$ and $\eta(a;\mu_1)$ should be equal to unity. This conservation condition for the number of neutrons is satisfied for all systems nearly completely, as seen from Table 2. Besides this, the results in the f_1-approximation are little different from those in the f_4-approximation, these being shown only for the smaller values of Σa in Table 3.

In this table, our results are compared with those in the Chandrasekhar's exact theory and in the Grosjean's approximation (Grosjean, 1958). It is clear that the results obtained by means of

our multiple collision method are very accurate. Although the results of $n_1(\tau_0,\mu;\mu_1)$ in the j_4-approximation reveal to have some error, as mentioned already, it is seen that this error hardly contributes to the total number, as expected, especially for the smaller Σa. (It is found out some difference between the results of $n_N(\tau_0,\mu;\mu_1)$ in the j_1- and j_4-approximation, but only a little difference between those of $n(\tau_0,\mu;\mu_1)$).

The total neutron current at the boundary of the slab, $J(\tau_0;\mu_1)$, is obtained in the j_1-approximation because we are convinced that the j_1-approximation gives an accurate result. The results are shown in Table 2. To interpret these results, the average cosine of the emission angle of the leakage neutrons is calculated:

$$|\mu(\tau_0;\mu_1)|_{av} = J(\tau_0;\mu_1)/n(\tau_0;\mu_1) . \tag{26}$$

The results in the j_1-approximation are shown also in Table 2. For the reflection, this value increases gradually from 1/2 to 2/3 as the value of Σa does. These asymptotic values correspond to the ones for the spherically symmetric emission and for the emission with a cosine distribution, that is, $n(0,\mu;\mu_1) \propto |\mu|$, respectively. Moreover, it is seen that the values of the average cosine decrease a little as the value of μ_1 does.

These are shown also analytically. According to Appendices I and II, Eqs. (13), (15) and (16) are written in the following forms, respectively, in the j_1-approximation:

$$\sum_{N=1}^{\infty} n_N(\tau_0,\mu;\mu_1) \sim \begin{cases} \frac{\alpha}{\mu_1}\left[1-\frac{\alpha}{\mu_1}-\frac{\alpha}{|\mu|}+\alpha\left(-\ln 2\alpha-\gamma+\frac{3}{2}\right)\right], & \frac{\alpha}{\mu_1},\frac{\alpha}{|\mu|}\to 0, \\ |\mu|\left[1\pm\left(1-\frac{\mu_1}{\alpha}-\frac{|\mu|}{\alpha}+\frac{1}{2\alpha^2}\right)\right], & \alpha\to\infty, \end{cases} \tag{27}$$

$$n(\tau_0;\mu_1)\sim\begin{cases}\frac{\alpha}{\mu_1}(1-\frac{\alpha}{\mu_1}),\\ 1-\frac{\alpha}{\mu_1},\end{cases}\qquad J(\tau_0;\mu_1)\sim\begin{cases}\frac{\alpha}{2\mu_1}\left[1-\frac{\alpha}{\mu_1}+\alpha(-\ln 2\alpha-\gamma-\frac{1}{2})\right],\\ \mu_1\left(1-\frac{2\alpha}{\mu_1}+\frac{\alpha}{2\mu_1^2}\right),\end{cases}\qquad \alpha/\mu_1\to 0, \tag{28}$$

$$\left.\begin{aligned} n(\tau_0;\mu_1)&\sim\tfrac{1}{2}\left[1\pm\left(1-\tfrac{2}{3\alpha}-\tfrac{\mu_1}{\alpha}+\tfrac{1}{2\alpha^2}+\tfrac{2\mu_1}{3\alpha^2}\right)\right],\\ J(\tau_0;\mu_1)&\sim\tfrac{1}{3}\left[1\pm\left(1-\tfrac{3}{4\alpha}-\tfrac{\mu_1}{\alpha}+\tfrac{1}{2\alpha^2}+\tfrac{3\mu_1}{4\alpha^2}\right)\right],\end{aligned}\right\}\quad \alpha\to\infty, \tag{29}$$

where $\alpha=\Sigma a/2$. And hence the average cosine in the j_1-approximation is given by

$$\left.\begin{aligned} |\mu(\tau_0;\mu_1)|_{av}&\sim\begin{cases}\frac{1}{2}\left[1+\alpha(-\ln 2\alpha-\gamma-1/2)\right], & \frac{\alpha}{\mu_1}\to 0,\\ \mu_1\left(1-\frac{\alpha}{\mu_1}+\frac{\alpha}{2\mu_1^2}\right),\end{cases}\\ &\sim\begin{cases}\frac{2}{3}\left(1-\frac{1}{2+4\alpha}\right), & \alpha\to\infty.\\ \frac{3}{4}\left(1+\frac{4\mu_1}{3}\right)/\left(1+\frac{3\mu_1}{2}\right),\end{cases}\end{aligned}\right\} \tag{30}$$

In the case of the transmission, the average cosine takes the value $\mu_1\left(1-\frac{\Sigma a}{3\mu_1}+\frac{\Sigma a}{4\mu_1^2}\right)$ asymptotically for small $\Sigma a/\mu_1$ and it tends to $\frac{3}{4}\left(1+\frac{4\mu_1}{3}\right)/\left(1+\frac{3\mu_1}{2}\right)$ as Σa increases indefinitely, as shown in Eq. (30). As seen from Table 2, these values have a maximum at the thickness $\Sigma a \simeq$ 100, 10 and 4 for the cases of that μ_1 = 1, 0.5 and 0.1, respectively. And they increase as the value of μ_1 decreases for large Σa, as guessed also from the last expression in Eq. (30). These are interpreted by considering that the smaller the value of μ_1 becomes, the farther the positions from which the transmitting neutrons mainly come, remove from the boundary.

The numerical results for the spherically symmetric source are shown in Figs. 27∼31 and Table 4. Figures 27 and 28 show the results of $n_N(0,\mu)$ in the j_4-approximation, where those for N = 1 are compared with the

exact ones which are obtained directly by integrating Eq. (6) for $N = 1$ with respect to μ_1. Here again, it is seen that the approximation gives an accurate result except that for $\Sigma a = 10$, which is underestimated a little. Comparing the results shown in Figs. 27 and 28 with those in Figs. 3 $\sim$ 12, it is seen that the former nearly coincides with the latter for the case of that $\mu_1 = 0.5$.

The results of $\eta_N(a,\mu)$ and $\eta(\tau_0,\mu)$ in the f_1-approximation are shown in Figs. 29, 30 and 31, respectively. It is seen also that these results are nearly the same as those for the monodirectional source with $\mu_1 = 0.5$ except those for $\eta_0(a,\mu)$, $\eta_0(a,\mu;\mu_1)$ being given by $\delta(\mu-\mu_1)\exp(-\Sigma a/\mu_1)$.

Table 4 shows the results of $\eta(\tau_0)$, $J(\tau_0)$ and $|\mu(\tau_0)|_{av}$ in the f_1-approximation. And the analytical expressions of them in the extreme cases are given as follows:

$$\sum_{N=1}^{\infty}\eta(\tau_0,\mu)\sim\begin{cases}\alpha(-\ln 2\alpha-\gamma+1+\frac{\alpha}{|\mu|}\ln 2\alpha), & \alpha/|\mu|\to 0,\\ |\mu|\left[1\pm\left(1-\frac{|\mu|}{\alpha}-\frac{1}{2\alpha}\right)\right], & \alpha\to\infty,\end{cases} \tag{31}$$

$$\left.\begin{aligned}\eta(\tau_0)&\sim\begin{cases}\alpha(-\ln 2\alpha-\gamma+1),\\ 1-\alpha(-\ln 2\alpha-\gamma+1),\end{cases}\\ J(\tau_0)&\sim\begin{cases}\alpha/2\,(-\ln 2\alpha-\gamma+1),\\ 1/2\,[1+\alpha(-\ln 2\alpha-\gamma-3)],\end{cases}\end{aligned}\right\}\quad \alpha\to 0, \tag{32}$$

$$\left.\begin{aligned}\eta(\tau_0)&\sim\tfrac{1}{2}\left[1\pm\left(1-\tfrac{7}{6\alpha}+\tfrac{1}{2\alpha^2}\right)\right],\\ J(\tau_0)&\sim\tfrac{1}{3}\left[1\pm\left(1-\tfrac{5}{4\alpha}+\tfrac{1}{2\alpha^2}\right)\right],\end{aligned}\right\}\quad \alpha\to\infty \tag{33}$$

$$\left.\begin{aligned}|\mu(\tau_0)|_{av}&\sim\begin{cases}1/2,\\ 1/2\,[1+2\alpha(-\ln 2\alpha-\gamma-1)],\end{cases}\quad \alpha\to 0,\\ &\sim\begin{cases}2/3\,(1-1/(24\alpha)),\\ 5/7\,(1+1/(35\alpha)),\end{cases}\quad \alpha\to\infty.\end{aligned}\right\} \tag{34}$$

4. Conclusions

The reflection and the transmission of neutrons for the homogeneous slab has been dealt with by a new analytical method, the multiple collision method.

In the constant cross section approximation, the expression for the number of leakage neutrons from the slab in a direction with μ as a result of the N-th collision of a monodirectional or spherically symmetric incident neutron, has be derived at first. And then the sum of this number over N and further the integration with respect to μ, the directional cosine of the emission angle, have been performed to get the total number of leakage neutrons. Moreover, the total neutron current at the surface of the slab, the so-called albedo for this slab and the average cosine of the emission angle of the leakage neutrons have been obtained.

Furthermore, it has been shown that these are easily extended to the case of that the cross section for the medium is assumed according to the two-group model. And the critical condition of the slab in the one-group approximation has been derived and shown that it coincides with the one obtained in the previous work.

The numerical results have been obtained by truncating the infinite sum in which all the above-mentioned expressions are written. By comparing some results with the exact ones, it has been shown that our results in the f_4-approximation, where only the first five terms in the infinite sum are taken into account, are very accurate especially for the slabs with the smaller values of Σa, the thickness measured in units of the total mean free path. Even in the f_1-approximation, the results for the quantities having been integrated with respect to μ, such as the total number of the leakage neutrons, are the most accurate among those obtained by using other approximate theories ever developed.

It is believed that the multiple collision method has, again in this report, revealed itself powerful and useful for obtaining accurate and plentiful information about neutron transport. Although the present work is performed under the assumption that the scattering of neutrons is spherically symmetric in the L system, the method will be extended to the case without this assumption. Moreover, it is hoped to perform a further extension of this technique to more general problems.

Acknowledgements. - The author wishes to express his gratitude to Dr. G. Blässer for his suggestion that the multiple collision method is to be applied to the present problem, and for his interest in this work.

REFERENCES

Asaoka T. (1961) - J. Atomic Energy Soc. Japan, 3, 531.

Asaoka T. and Nakahara Y. (1962) - Internal Report EURATOM, ISPRA-277.

Grosjean C. (1958) - Proc. Second Intern. Conf. Peaceful Uses Atomic Energy, Geneva. Paper P/1692.

APPENDIX I. Expressions of the Functions in Fig. 2

Concrete expressions of $j_n(-i\beta)e^{-\beta}$'s:

$$j_0(-i\beta)e^{-\beta} = \frac{1}{2\beta}(1-e^{-2\beta}),$$

$$j_1(-i\beta)e^{-\beta} = -\frac{1}{2\beta}\left[(1+e^{-2\beta})-\frac{1}{\beta}(1-e^{-2\beta})\right],$$

$$j_2(-i\beta)e^{-\beta} = -\frac{1}{2\beta}\left[(1-e^{-2\beta})-\frac{3}{\beta}(1+e^{-2\beta})+\frac{3}{\beta^2}(1-e^{-2\beta})\right],$$

$$j_3(-i\beta)e^{-\beta} = \frac{1}{2\beta}\left[(1+e^{-2\beta})-\frac{6}{\beta}(1-e^{-2\beta})+\frac{15}{\beta^2}(1+e^{-2\beta})-\frac{15}{\beta^3}(1-e^{-2\beta})\right],$$

$$j_4(-i\beta)e^{-\beta} = \frac{1}{2\beta}\left[(1-e^{-2\beta})-\frac{10}{\beta}(1+e^{-2\beta})+\frac{45}{\beta^2}(1-e^{-2\beta})-\frac{105}{\beta^3}(1+e^{-2\beta})+\frac{105}{\beta^4}(1-e^{-2\beta})\right].$$

Concrete expressions of $J(n,m)$'s:

$$J(0,0) = (1-\tfrac{1}{2}e^{-2\alpha})-\frac{1}{4\alpha}(1-e^{-2\alpha})+\alpha E_1(2\alpha),$$

$$J(1,1) = \frac{1}{3}-\frac{1}{4\alpha}-\frac{1}{4\alpha^2}e^{-2\alpha}+\frac{1}{8\alpha^3}(1-e^{-2\alpha}),$$

$$J(0,2) = \frac{1}{4\alpha}-\frac{1}{2\alpha^2}(1+\tfrac{1}{2}e^{-2\alpha})+\frac{3}{8\alpha^3}(1-e^{-2\alpha}),$$

$$J(2,2) = \frac{1}{5}-\frac{1}{4\alpha}+\frac{1}{4\alpha^2}e^{-2\alpha}+\frac{3}{8\alpha^3}(1+3e^{-2\alpha})+\frac{3}{2\alpha^4}e^{-2\alpha}-\frac{3}{4\alpha^5}(1-e^{-2\alpha}),$$

$$J(1,3) = \frac{1}{4\alpha}-\frac{5}{6\alpha^2}(1-\tfrac{3}{10}e^{-2\alpha})+\frac{9}{8\alpha^3}(1+\tfrac{11}{9}e^{-2\alpha})+\frac{5}{2\alpha^4}e^{-2\alpha}-\frac{5}{4\alpha^5}(1-e^{-2\alpha}),$$

$$J(3,3) = \frac{1}{7}-\frac{1}{4\alpha}-\frac{1}{4\alpha^2}e^{-2\alpha}+\frac{3}{4\alpha^3}(1-\tfrac{7}{2}e^{-2\alpha})-\frac{45}{4\alpha^4}e^{-2\alpha}-\frac{15}{4\alpha^5}(1+\tfrac{13}{2}e^{-2\alpha})-\frac{225}{8\alpha^6}e^{-2\alpha}$$
$$+\frac{225}{16\alpha^7}(1-e^{-2\alpha}),$$

$$J(0,4) = -\frac{1}{4\alpha}+\frac{5}{3\alpha^2}(1+\tfrac{3}{20}e^{-2\alpha})-\frac{45}{8\alpha^3}(1-\tfrac{17}{45}e^{-2\alpha})+\frac{21}{2\alpha^4}(1+\tfrac{3}{3}e^{-2\alpha})-\frac{35}{4\alpha^5}(1-e^{-2\alpha}),$$

$$J(2,4) = \frac{1}{4\alpha}-\frac{7}{6\alpha^2}(1+\tfrac{3}{14}e^{-2\alpha})+\frac{9}{4\alpha^3}(1-\tfrac{23}{18}e^{-2\alpha})-\frac{55}{4\alpha^4}e^{-2\alpha}-\frac{25}{4\alpha^5}(1+\tfrac{53}{10}e^{-2\alpha})-\frac{315}{8\alpha^6}e^{-2\alpha}$$
$$+\frac{315}{16\alpha^7}(1-e^{-2\alpha}),$$

$$J(4,4) = \frac{1}{9}-\frac{1}{4\alpha}+\frac{1}{4\alpha^2}e^{-2\alpha}+\frac{5}{4\alpha^3}(1+\tfrac{37}{10}e^{-2\alpha})+\frac{153}{4\alpha^4}e^{-2\alpha}-\frac{45}{4\alpha^5}(1-\tfrac{97}{6}e^{-2\alpha})+\frac{1305}{8\alpha^6}e^{-2\alpha}$$

$$+\frac{1575}{16\alpha^7}\left(1+\frac{51}{5}e^{-2\alpha}\right)+\frac{2205}{2\alpha^8}e^{-2\alpha}-\frac{2205}{4\alpha^7}\left(1-e^{-2\alpha}\right).$$

Concrete expressions of $\int_1^\infty \frac{dt}{t} j_n(-i\alpha t)e^{-\alpha t}$'s:

$$\int_1^\infty \frac{dt}{t} j_0(-i\alpha t)e^{-\alpha t}=\frac{1}{2\alpha}\left[1-E_2(2\alpha)\right],$$

$$\int_1^\infty \frac{dt}{t} j_1(-i\alpha t)e^{-\alpha t}=-\frac{i}{2\alpha}\left[1-\frac{1}{2\alpha}\left(1-e^{-2\alpha}\right)\right],$$

$$\int_1^\infty \frac{dt}{t} j_2(-i\alpha t)e^{-\alpha t}=-\frac{1}{2\alpha}\left[1-\frac{3}{2\alpha}\left(1+\frac{1}{3}e^{-2\alpha}\right)+\frac{1}{\alpha^2}\left(1-e^{-2\alpha}\right)\right],$$

$$\int_1^\infty \frac{dt}{t} j_3(-i\alpha t)e^{-\alpha t}=\frac{i}{2\alpha}\left[1-\frac{3}{\alpha}\left(1-\frac{1}{6}e^{-2\alpha}\right)+\frac{5}{\alpha^2}\left(1+\frac{1}{2}e^{-2\alpha}\right)-\frac{15}{4\alpha^3}\left(1-e^{-2\alpha}\right)\right],$$

$$\int_1^\infty \frac{dt}{t} j_4(-i\alpha t)e^{-\alpha t}=\frac{1}{2\alpha}\left[1-\frac{5}{\alpha}\left(1+\frac{1}{10}e^{-2\alpha}\right)+\frac{15}{\alpha^2}\left(1-\frac{3}{10}e^{-2\alpha}\right)-\frac{105}{4\alpha^3}\left(1+\frac{3}{5}e^{-2\alpha}\right)+\frac{21}{\alpha^4}\left(1-e^{-2\alpha}\right)\right].$$

Concrete expressions of $\int_1^\infty \frac{dt}{t^2} j_n(i\alpha t)e^{-\alpha t}$'s:

$$\int_1^\infty \frac{dt}{t^2} j_0(i\alpha t)e^{-\alpha t}=\frac{1}{4\alpha}\left[1-e^{-2\alpha}+2\alpha E_2(2\alpha)\right],$$

$$\int_1^\infty \frac{dt}{t^2} j_1(i\alpha t)e^{-\alpha t}=\frac{i}{4\alpha}\left[1+\frac{1}{3}e^{-2\alpha}-\frac{2}{3\alpha}\left(1-e^{-2\alpha}\right)-\frac{2}{3}\alpha E_2(2\alpha)\right],$$

$$\int_1^\infty \frac{dt}{t^2} j_2(i\alpha t)e^{-\alpha t}=-\frac{1}{4\alpha}\left[1-\frac{2}{\alpha}\left(1+\frac{1}{2}e^{-2\alpha}\right)+\frac{3}{2\alpha^2}\left(1-e^{-2\alpha}\right)\right],$$

$$\int_1^\infty \frac{dt}{t^2} j_3(i\alpha t)e^{-\alpha t}=-\frac{i}{4\alpha}\left[1-\frac{4}{\alpha}\left(1-\frac{1}{4}e^{-2\alpha}\right)+\frac{15}{2\alpha^2}\left(1+\frac{3}{5}e^{-2\alpha}\right)-\frac{6}{\alpha^3}\left(1-e^{-2\alpha}\right)\right],$$

$$\int_1^\infty \frac{dt}{t^2} j_4(i\alpha t)e^{-\alpha t}=\frac{1}{4\alpha}\left[1-\frac{20}{3\alpha}\left(1+\frac{3}{20}e^{-2\alpha}\right)+\frac{45}{2\alpha^2}\left(1-\frac{17}{45}e^{-2\alpha}\right)-\frac{42}{\alpha^3}\left(1+\frac{2}{3}e^{-2\alpha}\right)+\frac{35}{\alpha^4}\left(1-e^{-2\alpha}\right)\right].$$

Concrete expressions of $\int_1^\infty \frac{dt}{t^3} j_n(i\alpha t)e^{-\alpha t}$'s:

$$\int_1^\infty \frac{dt}{t^3} j_0(i\alpha t)e^{-\alpha t}=\frac{1}{6\alpha}\left[1-e^{-2\alpha}+2\alpha E_3(2\alpha)\right],$$

$$\int_1^\infty \frac{dt}{t^3} j_1(i\alpha t)e^{-\alpha t}=\frac{i}{6\alpha}\left[1+\frac{1}{2}e^{-2\alpha}-\frac{3}{4\alpha}\left(1-e^{-2\alpha}\right)-\alpha E_3(2\alpha)\right],$$

$$\int_1^\infty \frac{dt}{t^3} j_2(i\alpha t)e^{-\alpha t}=-\frac{1}{6\alpha}\left[1-\frac{1}{10}e^{-2\alpha}-\frac{9}{4\alpha}\left(1+\frac{3}{5}e^{-2\alpha}\right)+\frac{9}{5\alpha^2}\left(1-e^{-2\alpha}\right)+\frac{\alpha}{5}E_3(2\alpha)\right],$$

$$\int_1^\infty \frac{dt}{t^3} j_3(i\alpha t)e^{-\alpha t}=-\frac{i}{6\alpha}\left[1-\frac{9}{2\alpha}\left(1-\frac{1}{3}e^{-2\alpha}\right)+\frac{9}{\alpha^2}\left(1+\frac{2}{3}e^{-2\alpha}\right)-\frac{15}{2\alpha^3}\left(1-e^{-2\alpha}\right)\right],$$

$$\int_1^\infty \frac{dt}{t^3} j_4(i\alpha t)e^{-\alpha t}=\frac{1}{6\alpha}\left[1-\frac{15}{2\alpha}\left(1+\frac{1}{5}e^{-2\alpha}\right)+\frac{27}{\alpha^2}\left(1-\frac{1}{9}e^{-2\alpha}\right)-\frac{105}{2\alpha^3}\left(1+\frac{5}{7}e^{-2\alpha}\right)+\frac{315}{4\alpha^4}\left(1-e^{-2\alpha}\right)\right].$$

Leading terms of $j_n(-i\beta)e^{\beta}$'s for small β :

$$j_0(-i\beta)e^{\beta}\sim 1-\beta+\frac{2}{3}\beta^2-\frac{1}{3}\beta^3,\quad j_1(-i\beta)e^{\beta}\sim -\frac{i}{3}\beta\left(1-\beta+\frac{3}{5}\beta^2-\frac{4}{15}\beta^3\right),$$

$$j_2(-i\beta)e^{\beta}\sim -\frac{1}{15}\beta^2\left(1-\beta+\frac{4}{7}\beta^2-\frac{5}{21}\beta^3\right),\quad j_3(-i\beta)e^{\beta}\sim \frac{i}{105}\beta^3\left(1-\beta+\frac{5}{9}\beta^2-\frac{6}{27}\beta^3\right),$$

$$j_4(-i\beta)e^{\beta}\sim \frac{1}{945}\beta^4\left(1-\beta+\frac{6}{11}\beta^2-\frac{7}{33}\beta^3\right).$$

Leading terms of $J(n,m)$'s for small α (γ ; the Euler-Mascheroni constant):

$$J(0,0)\sim\alpha\left(-\ln 2\alpha-\gamma+\frac{3}{2}\right)+\frac{2}{3}\alpha^2-\frac{1}{6}\alpha^3,\quad J(1,1)\sim\frac{1}{4}\alpha-\frac{2}{15}\alpha^2+\frac{1}{18}\alpha^3-\frac{2}{105}\alpha^4,$$

$$J(0,2)\sim\frac{1}{12}\alpha-\frac{1}{15}\alpha^2+\frac{1}{30}\alpha^3-\frac{4}{315}\alpha^4,\quad J(2,2)\sim\frac{1}{12}\alpha-\frac{2}{105}\alpha^2+\frac{2}{945}\alpha^4,$$

$$J(1,3)\sim\frac{1}{36}\alpha-\frac{1}{125}\alpha^2,\quad J(3,3)\sim\frac{1}{27}\alpha-\frac{2}{315}\alpha^2,$$

$$J(0,4)\sim-\frac{1}{180}\alpha+O(\alpha^3),\quad J(2,4)\sim\frac{1}{72}\alpha-\frac{1}{315}\alpha^2,$$

$$J(4,4)\sim\frac{1}{40}\alpha-\frac{2}{693}\alpha^2+O(\alpha^4).$$

Leading terms of $\int_1^\infty\frac{dt}{t}j_n(-i\alpha t)e^{-\alpha t}$'s, $\int_1^\infty\frac{dt}{t^2}j_n(i\alpha t)e^{-\alpha t}$'s and $\int_1^\infty\frac{dt}{t^3}j_n(i\alpha t)e^{-\alpha t}$'s for small α :

n	$\int_1^\infty\frac{dt}{t}j_n(-i\alpha t)e^{-\alpha t}$	$\int_1^\infty\frac{dt}{t^2}j_n(i\alpha t)e^{-\alpha t}$	$\int_1^\infty\frac{dt}{t^3}j_n(i\alpha t)e^{-\alpha t}$
0	$-\ln 2\alpha-\gamma+1+\alpha-\frac{1}{3}\alpha^2$	$1-\alpha\left(-\ln 2\alpha-\gamma+\frac{3}{2}\right)-\frac{2}{3}\alpha^2+\frac{1}{6}\alpha^3$	$\frac{1}{2}-\alpha+\frac{2}{3}\alpha^2\left(-\ln 2\alpha-\gamma+\frac{11}{6}\right)+\frac{1}{3}\alpha^3$
1	$-\frac{1}{2}\left(1-\frac{2}{3}\alpha+\frac{1}{3}\alpha^2\right)$	$\frac{1}{3}\alpha\left(-\ln 2\alpha-\gamma+\frac{5}{6}+\alpha-\frac{3}{10}\alpha^2\right)$	$\frac{1}{3}\alpha\left[1-\alpha\left(-\ln 2\alpha-\gamma+\frac{19}{12}\right)-\frac{3}{5}\alpha^2\right]$
2	$-\frac{1}{6}\left(1-\frac{1}{5}\alpha^2\right)$	$-\frac{1}{12}\alpha\left(1-\frac{4}{5}\alpha+\frac{2}{5}\alpha^2\right)$	$-\frac{1}{15}\alpha^2\left(-\ln 2\alpha-\gamma+\frac{47}{60}\right)$
3	$\frac{1}{12}\left(1+O(\alpha^3)\right)$	$-\frac{1}{60}\alpha\left(1-\frac{3}{7}\alpha^2\right)$	$-\frac{1}{70}\alpha^2$
4	$\frac{1}{30}\left(1+O(\alpha^3)\right)$	$\frac{1}{180}\alpha\left(1-\frac{1}{13}\alpha^3\right)$	$\frac{1}{630}\alpha^2$

APPENDIX II. Expressions of $f_n(\mu_1)$'s up to in the j_4-approximation

Expression of $f_0(\mu_1)$ in the j_0 - and j_1-approximations:

$$f_0(\mu_1)=\frac{1}{C}f_0^2(\mu_1)\Big/\left[\frac{1}{C}-J(0,0)\right].$$

Expression of $f_1(\mu_1)$ in the j_1 - and j_2-approximations:

$$f_1(\mu_1)=\frac{1}{3C}f_1^2(\mu_1)\Big/\left[\frac{1}{3C}-J(1,1)\right].$$

Expressions of $f_0(\mu_1)$ and $f_2(\mu_1)$ in the j_2 - and j_3-approximations:

$$f_0(\mu_1)=\left[\frac{1}{C}f_0^2(\mu_1)\left(\frac{1}{5C}-J(2,2)\right)+\frac{1}{5C}f_2^2(\mu_1)J(0,2)\right]\Big/\left[\left(\frac{1}{C}-J(0,0)\right)\left(\frac{1}{5C}-J(2,2)\right)-(J(0,2))^2\right],$$

$$f_2(\mu_1)=\left[\frac{1}{C}f_0^2(\mu_1)J(0,2)+\frac{1}{5C}f_2^2(\mu_1)\left(\frac{1}{C}-J(0,0)\right)\right]\Big/\left[\left(\frac{1}{C}-J(0,0)\right)\left(\frac{1}{5C}-J(2,2)\right)-(J(0,2))^2\right],$$

and the leading terms of the denominator for $C = 1$ are given by

$$\left(1-J(0,0)\right)\left(\frac{1}{5}-J(2,2)\right)-(J(0,2))^2\sim\begin{cases}\frac{1}{5}\left[1-\alpha\left(-\ln 2\alpha-\gamma+\frac{23}{12}\right)\right], & \alpha\to 0,\\ \frac{1}{4\alpha^3}\left(1-\frac{17}{8\alpha}+\frac{3}{2\alpha^2}\right), & \alpha\to\infty.\end{cases}$$

Expressions of $f_1(\mu_1)$ and $f_3(\mu_1)$ in the j_3 - and j_4-approximations:

$$f_1(\mu_1)=\left[\frac{1}{3C}f_1^2(\mu_1)\left(\frac{1}{7C}-J(3,3)\right)+\frac{1}{7C}f_3^2(\mu_1)J(1,3)\right]\Big/\left[\left(\frac{1}{3C}-J(1,1)\right)\left(\frac{1}{7C}-J(3,3)\right)-(J(1,3))^2\right],$$

$$f_3(\mu_1)=\left[\frac{1}{3C}f_1^2(\mu_1)J(1,3)+\frac{1}{7C}f_3^2(\mu_1)\left(\frac{1}{3C}-J(1,1)\right)\right]\Big/\left[\left(\frac{1}{3C}-J(1,1)\right)\left(\frac{1}{7C}-J(3,3)\right)-(J(1,3))^2\right],$$ and

the leading terms of the denominator for $C = 1$ are given by

$$\left(\frac{1}{3}-J(1,1)\right)\left(\frac{1}{7}-J(3,3)\right)-(J(1,3))^2\sim\begin{cases}\frac{1}{21}\left(1-\frac{25}{24}\alpha\right), & \alpha\to 0,\\ \frac{5}{12\alpha^3}\left(1-\frac{85}{24\alpha}\right), & \alpha\to\infty.\end{cases}$$

Expressions of $f_0(\mu_1)$, $f_2(\mu_1)$ and $f_4(\mu_1)$ in the f_4-approximat

$$f_0(\mu_1)=\frac{1}{D}\Big\{\frac{1}{c}f_0^2(\mu_1)\big[\big(\tfrac{1}{5c}-J(2,2)\big)\big(\tfrac{1}{9c}-J(4,4)\big)-\big(J(2,4)\big)^2\big]$$
$$+\frac{1}{5c}f_2^2(\mu_1)\big[J(0,2)\big(\tfrac{1}{9c}-J(4,4)\big)+J(0,4)J(2,4)\big]+\frac{1}{9c}f_4^2(\mu_1)\big[J(0,2)J(2,4)+J(0,4)\big(\tfrac{1}{5c}-J(2,2)\big)\big]\Big\},$$

$$f_2(\mu_1)=\frac{1}{D}\Big\{\frac{1}{c}f_0^2(\mu_1)\big[J(0,2)\big(\tfrac{1}{9c}-J(4,4)\big)+J(0,4)J(2,4)\big]$$
$$+\frac{1}{5c}f_2^2(\mu_1)\big[\big(\tfrac{1}{c}-J(0,0)\big)\big(\tfrac{1}{9c}-J(4,4)\big)-\big(J(0,4)\big)^2\big]+\frac{1}{9c}f_4^2(\mu_1)\big[J(2,4)\big(\tfrac{1}{c}-J(0,0)\big)+J(0,2)J(0,4)\big]\Big\},$$

$$f_4(\mu_1)=\frac{1}{D}\Big\{\frac{1}{c}f_0^2(\mu_1)\big[J(0,2)J(2,4)+J(0,4)\big(\tfrac{1}{5c}-J(2,2)\big)\big]$$
$$+\frac{1}{5c}f_2^2(\mu_1)\big[J(2,4)\big(\tfrac{1}{c}-J(0,0)\big)+J(0,2)J(0,4)\big]+\frac{1}{9c}f_4^2(\mu_1)\big[\big(\tfrac{1}{c}-J(0,0)\big)\big(\tfrac{1}{5c}-J(2,2)\big)-\big(J(0,2)\big)^2\big]\Big\},$$

where

$$D=\big(\tfrac{1}{9c}-J(4,4)\big)\big[\big(\tfrac{1}{c}-J(0,0)\big)\big(\tfrac{1}{5c}-J(2,2)\big)-\big(J(0,2)\big)^2\big]-\big(J(2,4)\big)^2\big(\tfrac{1}{c}-J(0,0)\big)$$
$$-\big(J(0,4)\big)^2\big(\tfrac{1}{5c}-J(2,2)\big)-2J(0,2)J(0,4)J(2,4),$$

and the leading terms of each factor and the denominator D for $c=1$, for small α and for large α, are written in the following forms, respectively:

$\big(\frac{1}{5}-J(2,2)\big)\big(\frac{1}{9}-J(4,4)\big)-\big(J(2,4)\big)^2 \sim \frac{1}{45}\big(1-\frac{99}{140}\alpha\big)$ and $\frac{7}{120\alpha^3}\big(1-\frac{119}{24\alpha}+\frac{9}{\alpha^2}\big)$,

$J(0,2)\big(\frac{1}{9}-J(4,4)\big)+J(0,4)J(2,4) \sim \frac{1}{108}\alpha\big(1-\frac{31}{30}\alpha\big)$ and $\frac{7}{120\alpha^3}\big(1-\frac{85}{120\alpha}+\frac{93}{40\alpha^2}\big)$,

$J(0,2)J(2,4)+J(0,4)\big(\frac{1}{5}-J(2,2)\big) \sim -\frac{1}{900}\alpha\big(1-\frac{35}{24}\alpha\big)$ and $-\frac{7}{96\alpha^4}\big(1-\frac{6}{\alpha}\big)$,

$\big(1-J(0,0)\big)\big(\frac{1}{9}-J(4,4)\big)-\big(J(0,4)\big)^2 \sim \frac{1}{9}\big[1-\alpha\big(-\ln 2\alpha-\gamma+\frac{69}{70}\big)\big]$ and $\frac{5}{6\alpha^3}\big(1-\frac{85}{120\alpha}+\frac{144}{50\alpha^2}\big)$,

$J(2,4)\big(1-J(0,0)\big)+J(0,2)J(0,4) \sim \frac{1}{72}\alpha\big[1-\alpha\big(-\ln 2\alpha-\gamma+\frac{23}{15}\big)\big]$ and $\frac{1}{16\alpha^3}\big(1-\frac{85}{120\alpha}+\frac{97}{40\alpha^2}\big)$,

$D \sim \frac{1}{45}\big[1-\alpha\big(-\ln 2\alpha-\gamma+\frac{307}{140}\big)\big]$ and $\frac{7}{120\alpha^3}\big(1-\frac{85}{120\alpha}\big)$.

Table 1 - List of numerical results

Item	Range of parameters			Numerical results are shown in
	Number of collisions N	Absolute value of directional cosine of leakage neutron, $\|\mu\|$	Slab thickness Σa	
$\eta_N(\chi_0;\mu;\mu_1)$	0~70	0.1,0.3,0.5, 0.8 and 1	0.5,1,2,4 and 10	Figs. 3~24
$\eta(\chi_0;\mu;\mu_1)$	--	"	"	Figs. 25 and 26
$\eta(\chi_0;\mu_1)$	--	--	0.01~100	Table 2
$J(\chi_0;\mu_1)$	--	--	"	"
$\|\mu(\chi_0;\mu_1)\|_{av}^{*}$	--	--	"	"
$\eta_N(\chi_0;\mu)$	0~100	0.1,0.3,0.5, 0.8 and 1	0.5,1,2,4 and 10	Figs. 27~30
$\eta(\chi_0;\mu)$	--	"	"	Fig. 31
$\eta(\chi_0)$	--	--	"	Table 4
$J(\chi_0)$	--	--	"	"
$\|\mu(\chi_0)\|_{av}^{*}$	--	--	"	"

* The average cosine of the emission angle of the leakage neutrons (see Eq.(26)).

Table 2 - Total number of neutrons leaking from the slab in the j_+-approximation, total neutron current at the surface and average cosine of the emission angle of the leakage neutrons in the j_--approximation (monodirectional source)

(to be continued)

Slab thickness Σa	$n(0;\mu_1)$			$n(a;\mu_1)$			$J(0;\mu_1)$			$J(a;\mu_1)$		
	$\mu_1 = 1$	0.5	0.1	$\mu_1 = 1$	0.5	0.1	$\mu_1 = 1$	0.5	0.1	$\mu_1 = 1$	0.5	0.1
0.01	0.004975	0.009902	0.04760	0.99503	0.99010	0.95240	0.002533	0.005041	0.02423	0.99258	0.49514	0.11471
0.1	0.04769	0.09104	0.32307	0.95231	0.90896	0.67693	0.02595	0.04950	0.17440	0.93072	0.45860	0.20671
0.5	0.20251	0.33438	0.60494	0.79749	0.66562	0.39506	0.12142	0.19920	0.34908	0.72268	0.36640	0.25130
1	0.34133	0.49838	0.69756	0.65867	0.50162	0.30244	0.21349	0.30851	0.41908	0.55486	0.30694	0.21443
2	0.51753	0.65722	0.78825	0.48247	0.34278	0.21181	0.33361	0.41937	0.49410	0.36909	0.23393	0.16207
4	0.69098	0.78560	0.86551	0.30902	0.21441	0.13450	0.45271	0.51197	0.55977	0.21892	0.15348	0.10573
10	0.85322	0.89824	0.93485	0.14679	0.10176	0.06515	0.56464	0.59356	0.61669	0.10204	0.07311	0.04998
20	0.92189	0.94568	0.96480	0.07811	0.05432	0.03520	0.61223	0.62772	0.64012	0.05444	0.03894	0.02655
100	0.98355	0.98850	0.99246	0.01644	0.01149	0.007527	0.65516	0.65845	0.66108	0.01150	0.008218	0.005591

Table 2 (Continued)

Slab thickness Σa	$-\mu(0;\mu_1)_{av}$			$\mu(a;\mu_1)_{av}$		
	$\mu_1 = 1$	0.5	0.1	$\mu_1 = 1$	0.5	0.1
0.01	0.5092	0.5092	0.5091	0.9976	0.5001	0.1204
0.1	0.5442	0.5437	0.5398	0.9773	0.5045	0.3054
0.5	0.5996	0.5957	0.5775	0.9062	0.5505	0.6353
1	0.6254	0.6190	0.6027	0.8424	0.6120	0.7039
2	0.6444	0.6380	0.6302	0.7653	0.6826	0.7502
4	0.6546	0.6519	0.6498	0.7098	0.7151	0.7633
10	0.6614	0.6610	0.6607	0.6977	0.7165	0.7497
20	0.6639	0.6639	0.6638	0.6989	0.7154	0.7441
100	0.6661	0.6661	0.6661	0.6998	0.7145	0.7401

Table 3 - Comparison of the total number of neutrons transmitting the slab.

Directional cosine of incident neutron μ_1	Slab thickness Σa	Chandrasekhar's exact theory	Grosjean's approximation	Our j_4-approximation	Our j_1-approximation
1	0.1	0.9523	0.9523	0.95231	0.95231
	0.5	0.7974	0.7968	0.79749	0.79749
	1	0.6590	0.6565	0.65867	0.65863
0.5	0.1	0.9089	0.9089	0.90896	0.90896
	0.5	0.6654	0.6634	0.66562	0.66561
	1	0.5018	0.4960	0.50162	0.50157

Table 4 - Total number of neutrons leaking from the slab, $n(\chi_0)$, total neutron current at the surface, $J(\chi_0)$, and average cosine of the emission angle of the leakage neutrons in the f_1-approximation (isotropic source)

Slab thickness	Σa=0.5	1	2	4	10
$n(0)$	0.37437	0.51559	0.66035	0.78553	0.89796
$n(a)$	0.62563	0.48441	0.33965	0.21447	0.10204
$J(0)$	0.22049	0.31678	0.42048	0.51201	0.59356
$J(a)$	0.40767	0.33237	0.24119	0.15412	0.07311
$-\mu(0)_{av}$	0.5890	0.6144	0.6368	0.6518	0.6610
$\mu(a)_{av}$	0.6516	0.6861	0.7101	0.7186	0.7165

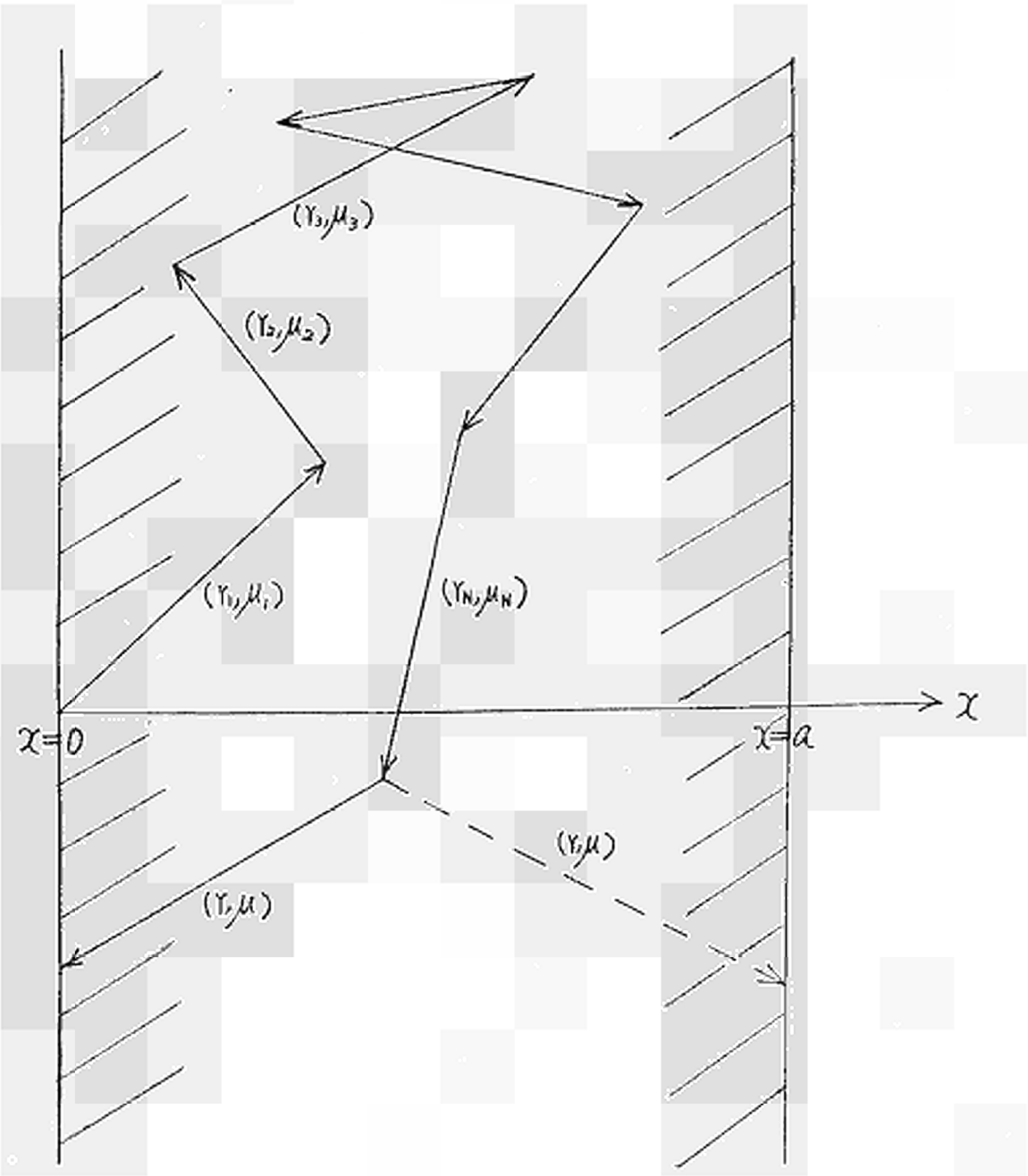

Fig. 1 - A typical path of the incident neutron in the slab

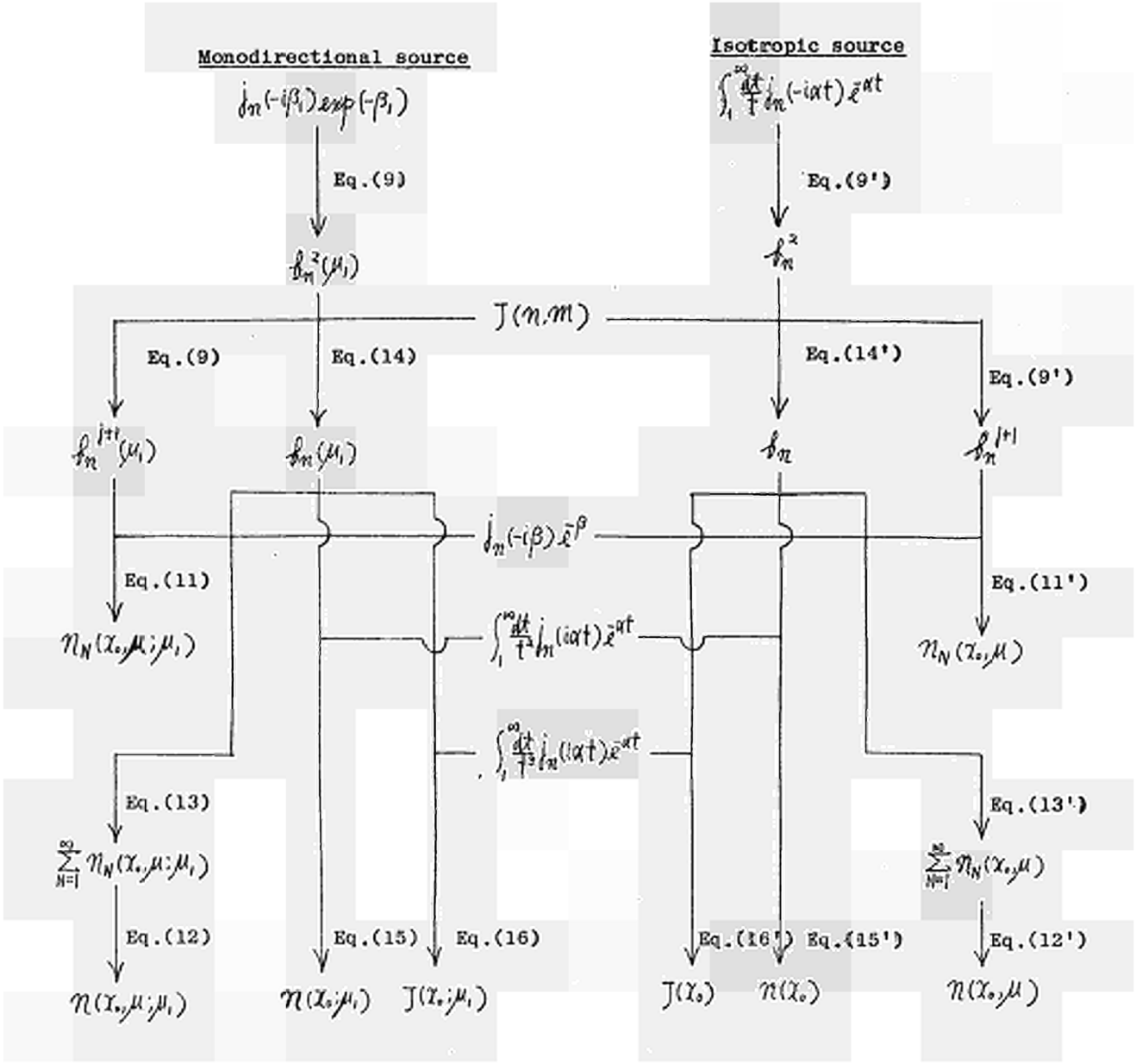

Fig. 2 - Flow diagram of calculations in the constant cross section approximation

Fig. 3 – Number of neutrons reflected after the first collision (monodirectional source)

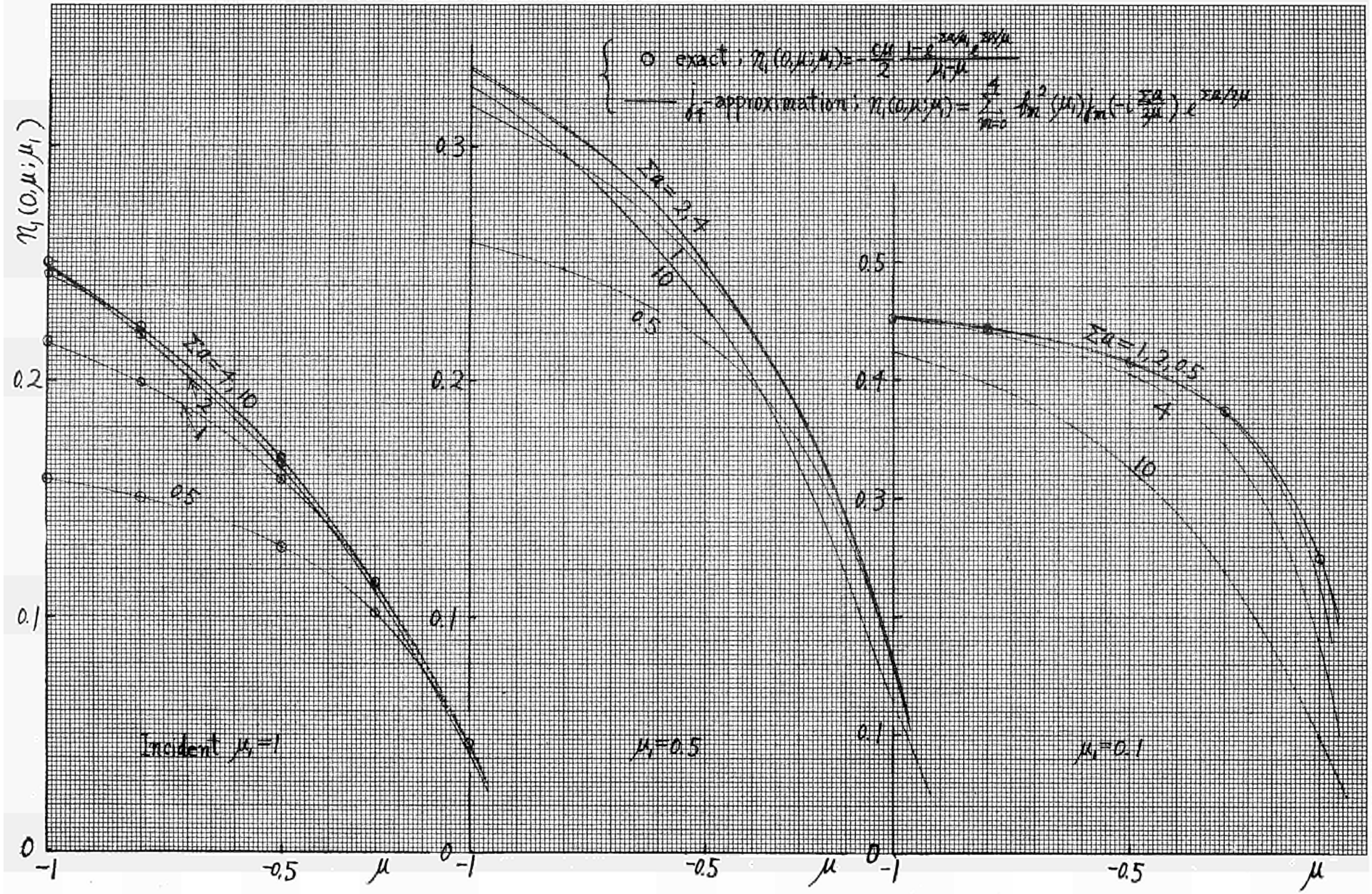

Fig. 4 — Number of neutrons reflected after the second collision (monodirectional source)

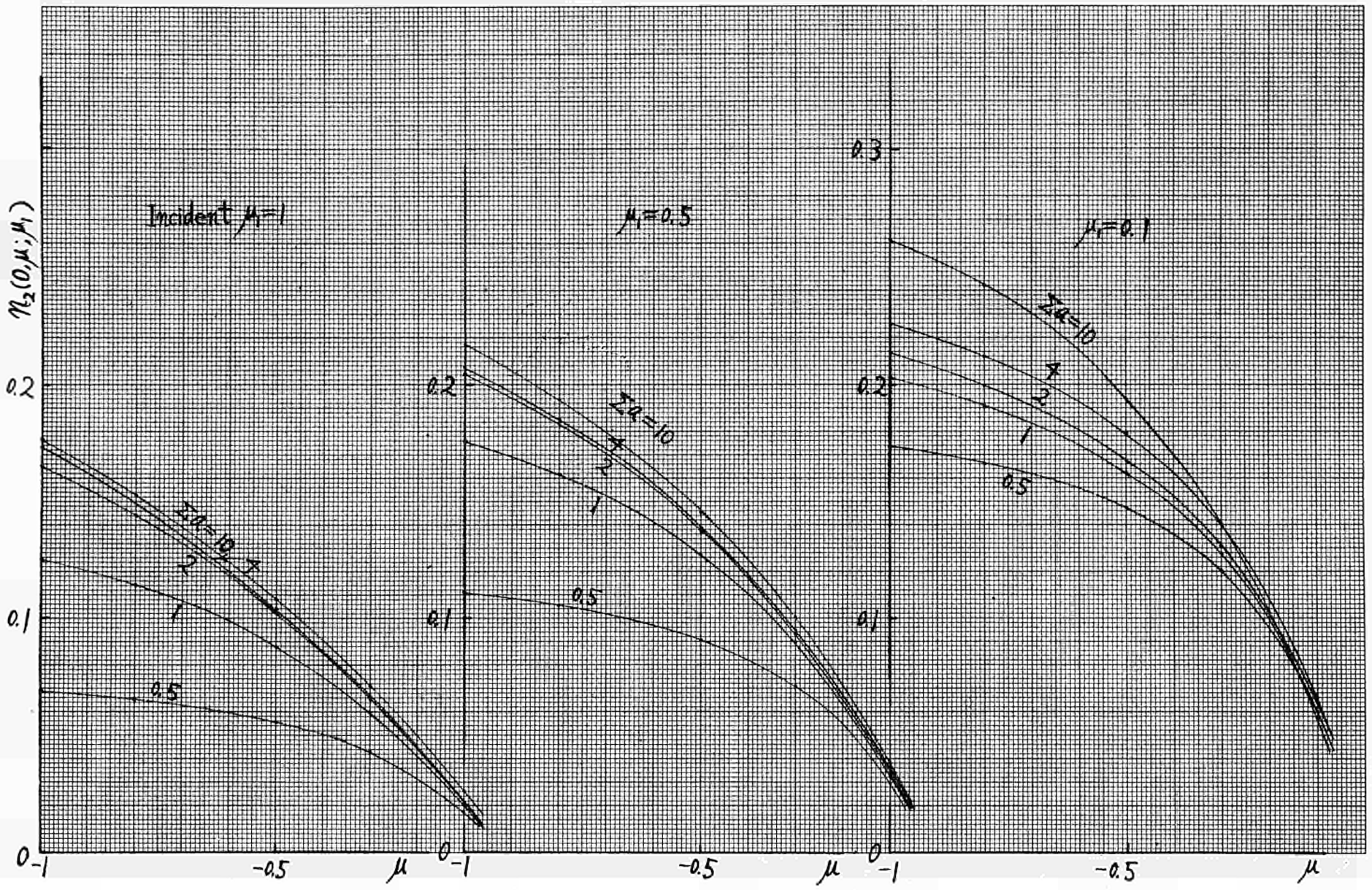

Fig. 5 — Number of neutrons reflected after the third collision (monodirectional source)

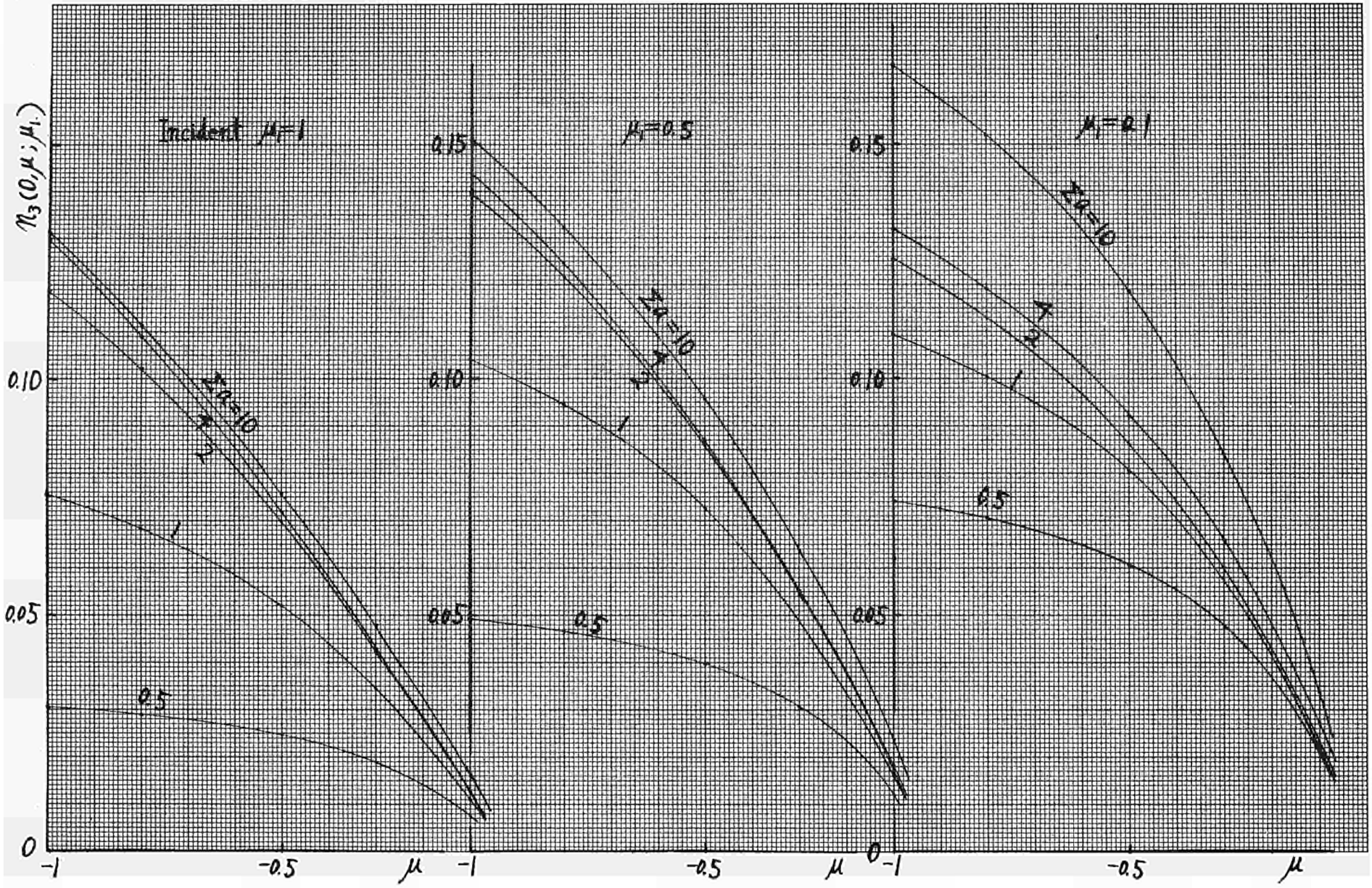

Fig. 6 — Number of neutrons reflected after the 5-th collision (monodirectional source)

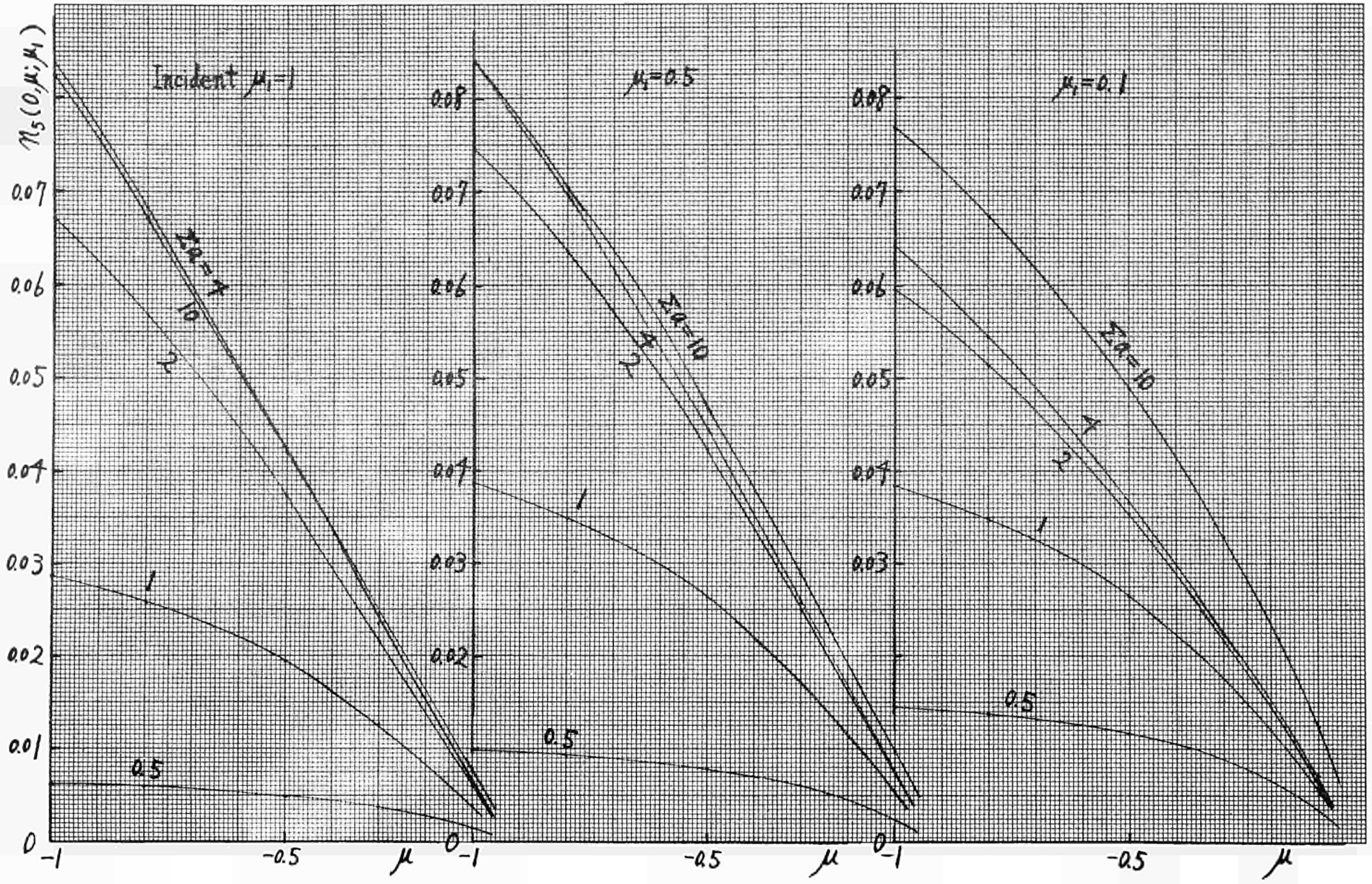

Fig. 7 — Number of neutrons reflected after the 7-th collision (monodirectional source)

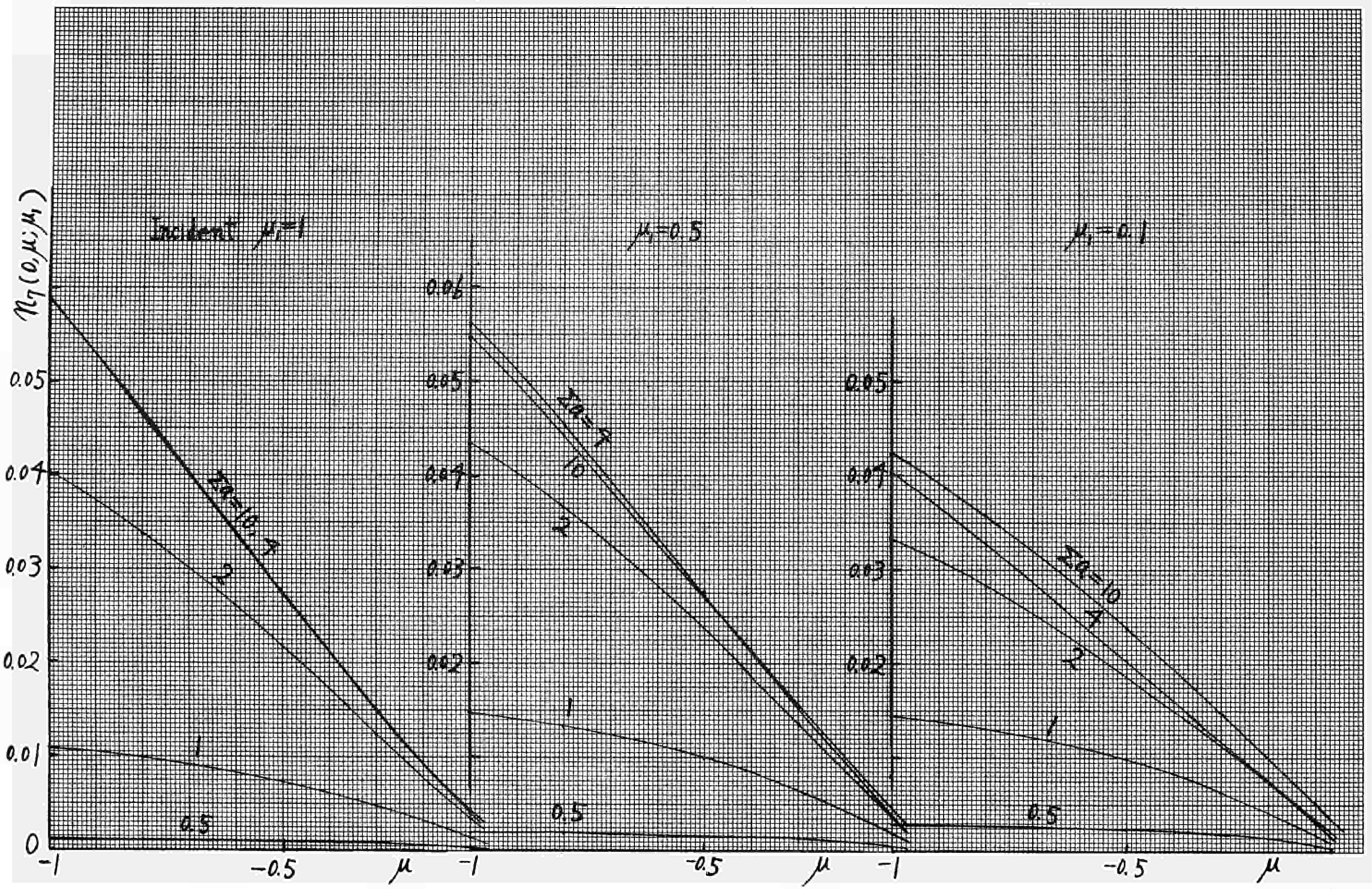

Fig. 8 — Number of neutrons reflected after the 10-th collision (monodirectional source)

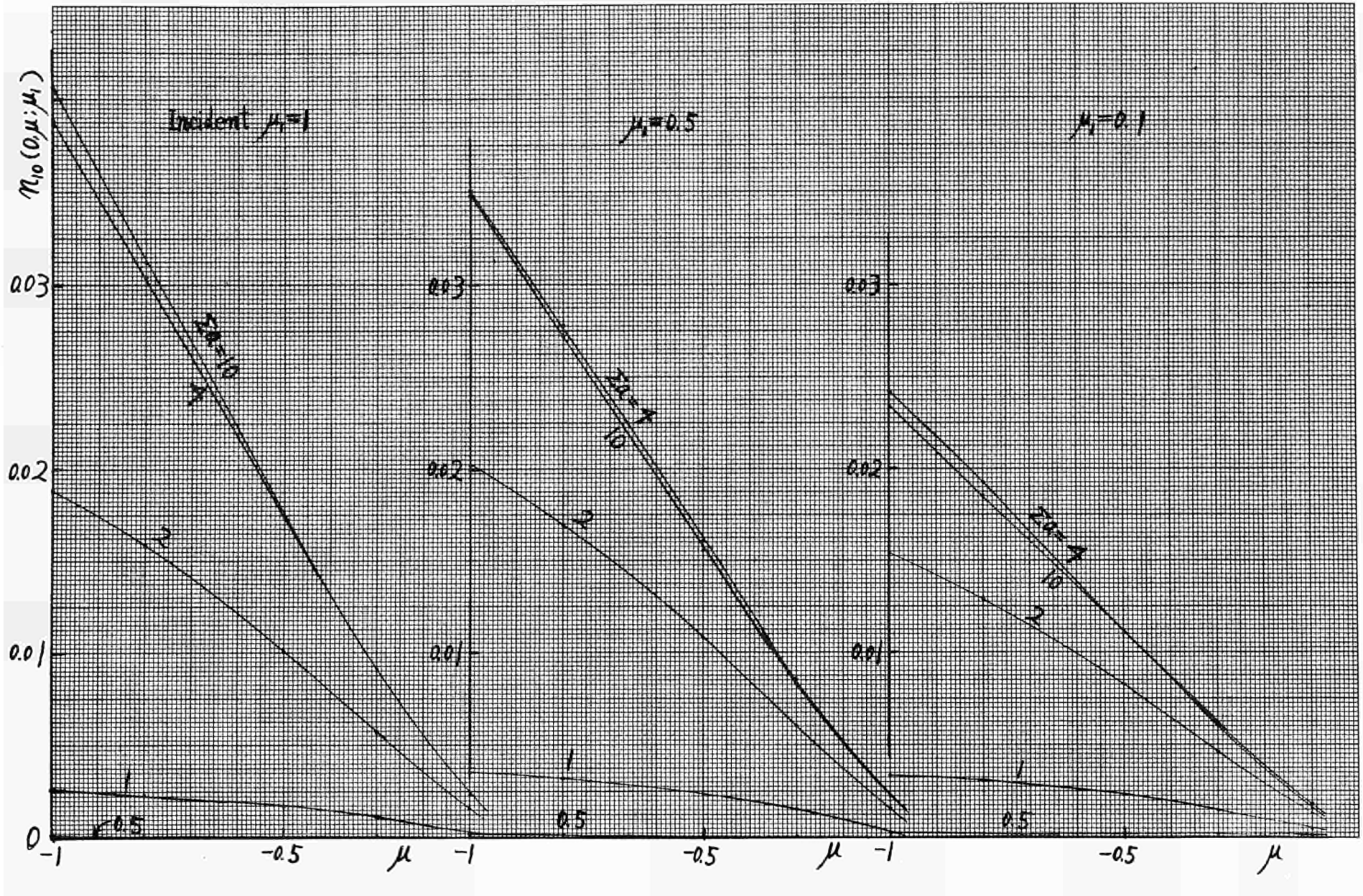

Fig. 9 — Number of neutrons reflected after the 15-th collision (monodirectional source)

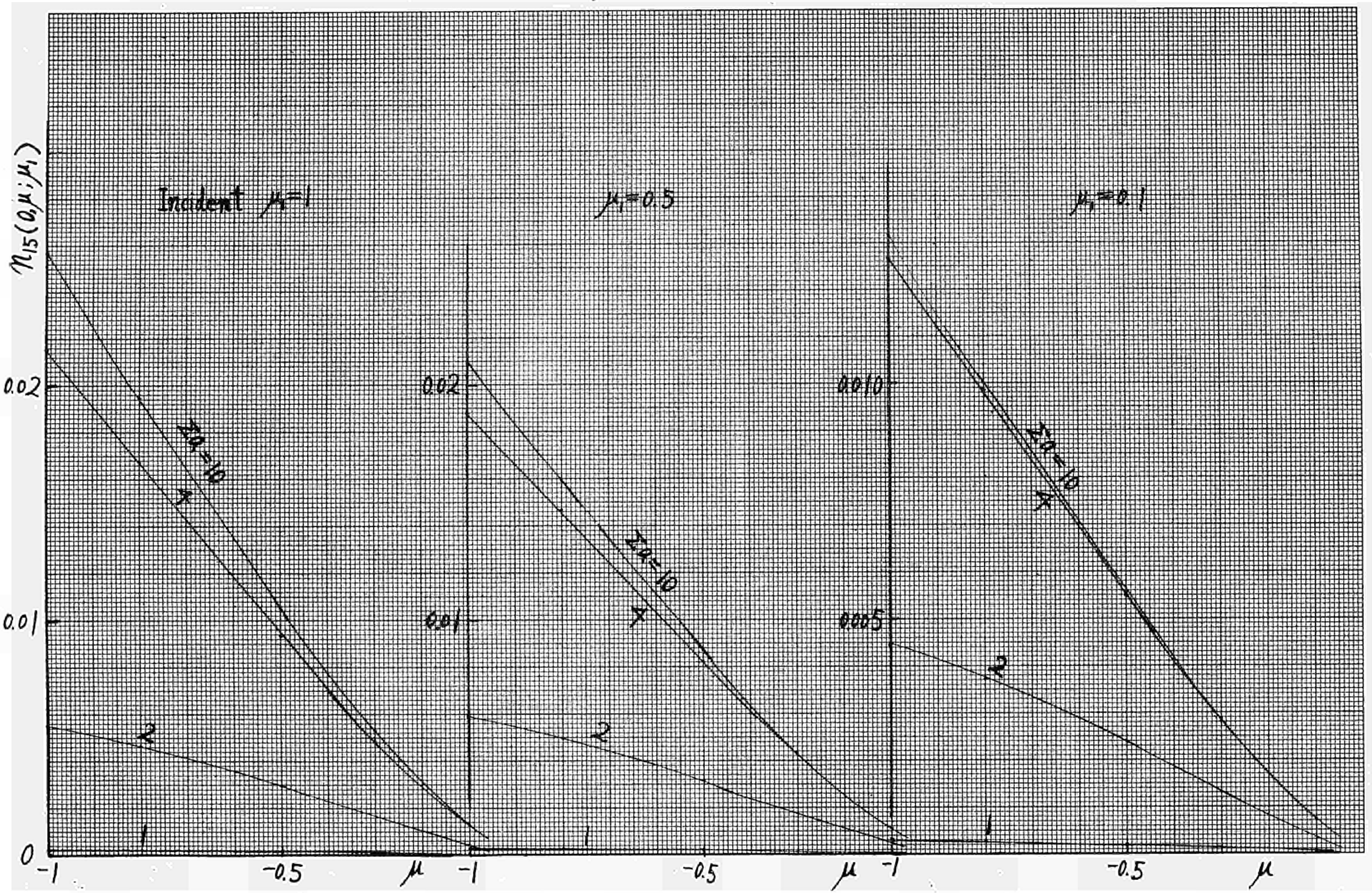

Fig. 10 — Number of neutrons reflected after the 20-th collision (monodirectional source)

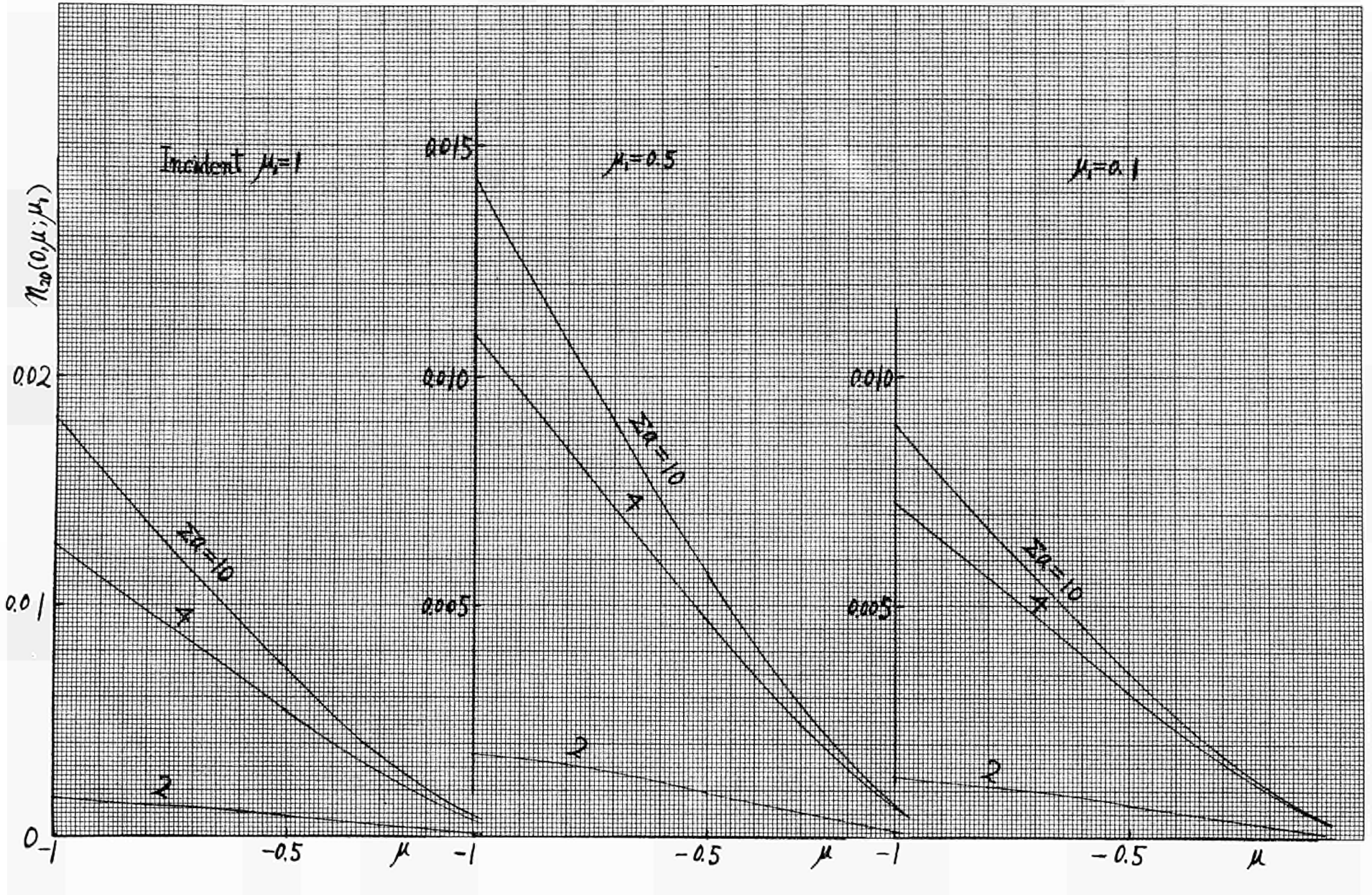

Fig. 11 – Number of neutrons reflected after the 30-th collision (monodirectional source)

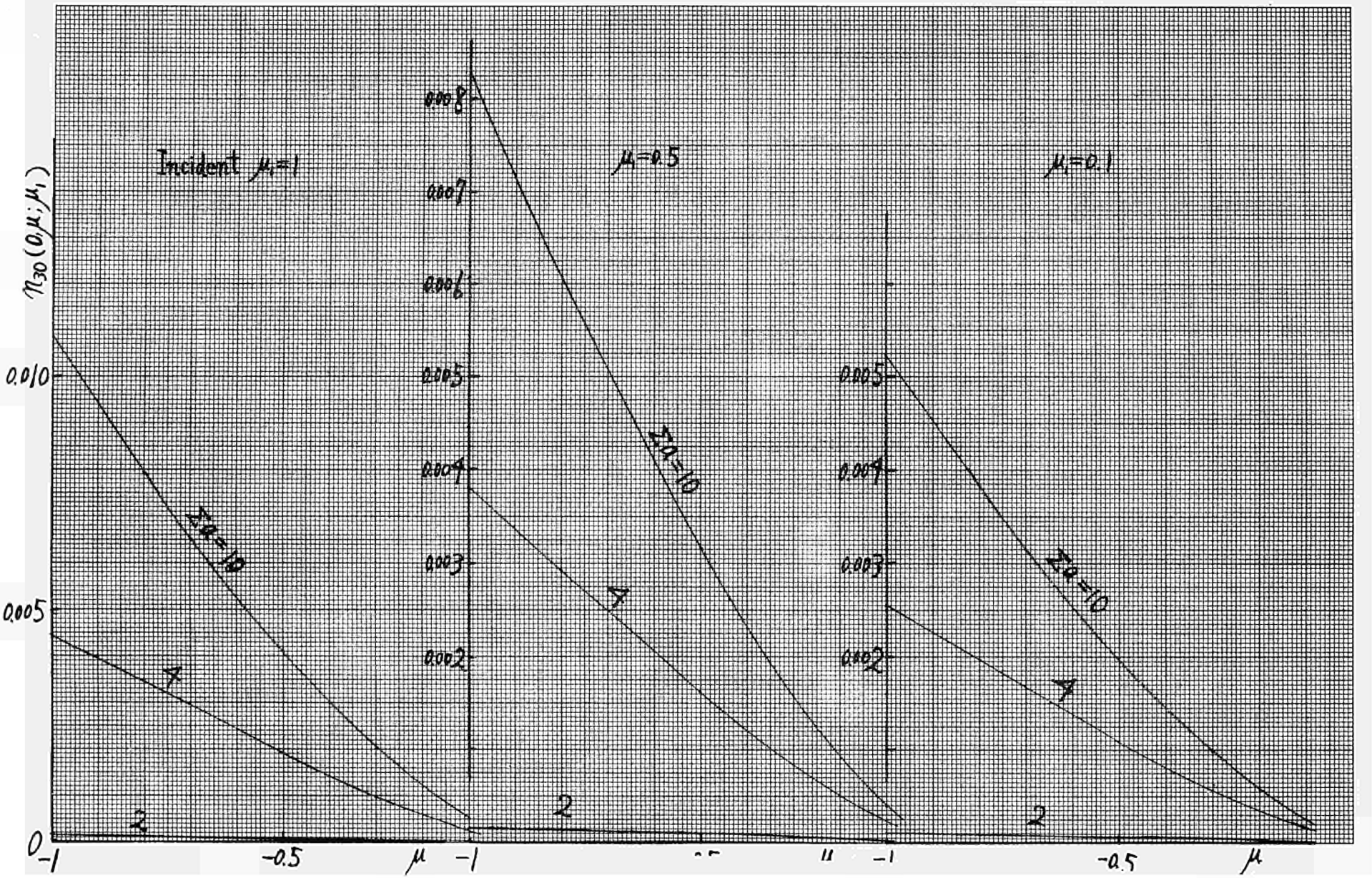

Fig. 12 — Number of neutrons reflected after the 50-th or the 70-th collision (monodirectional source)

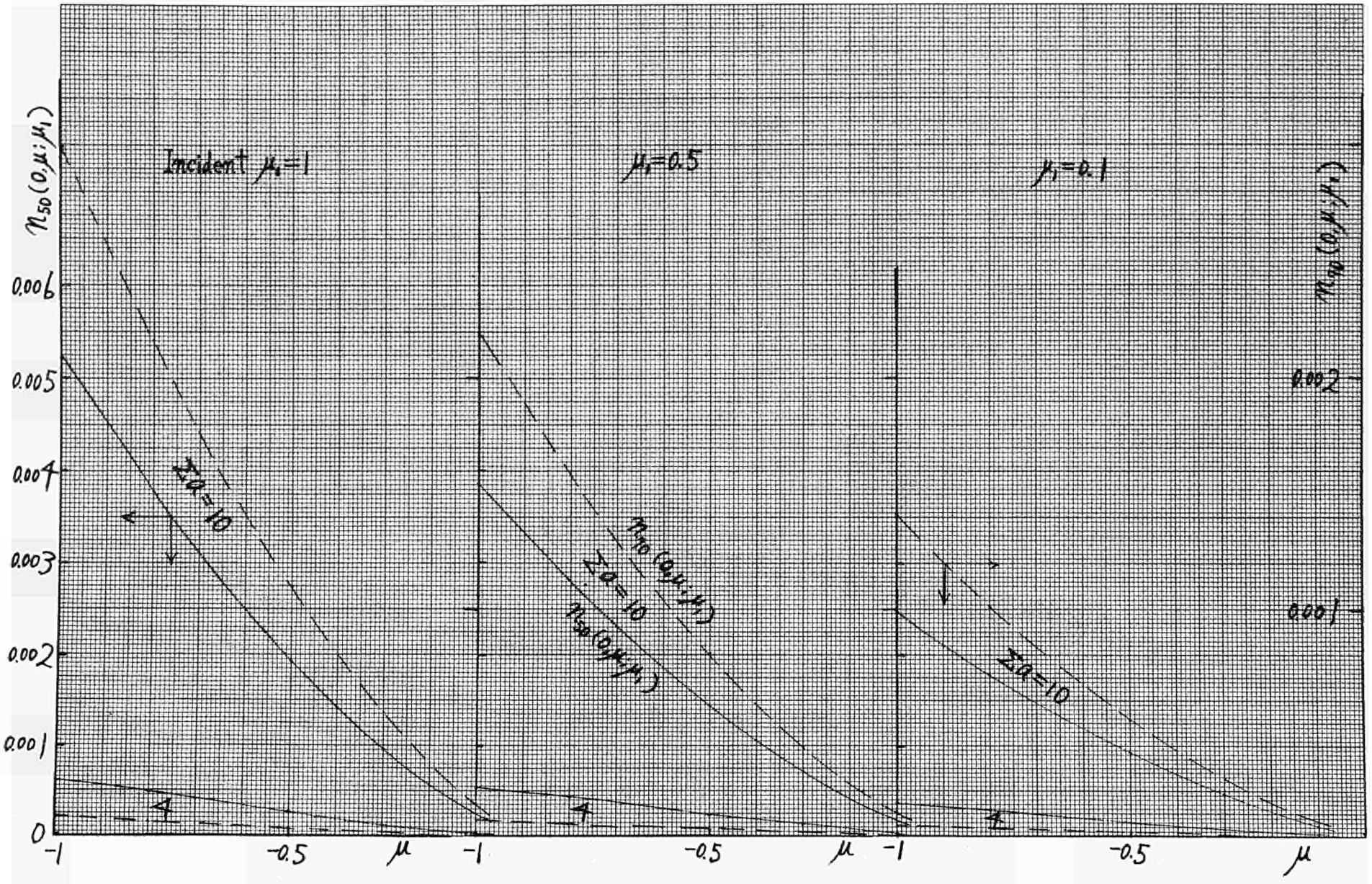

Fig. 13 — Number of neutrons reflected by the slab with $\Sigma a = 2$ or 4 after the N-th collision (monodirectional source)

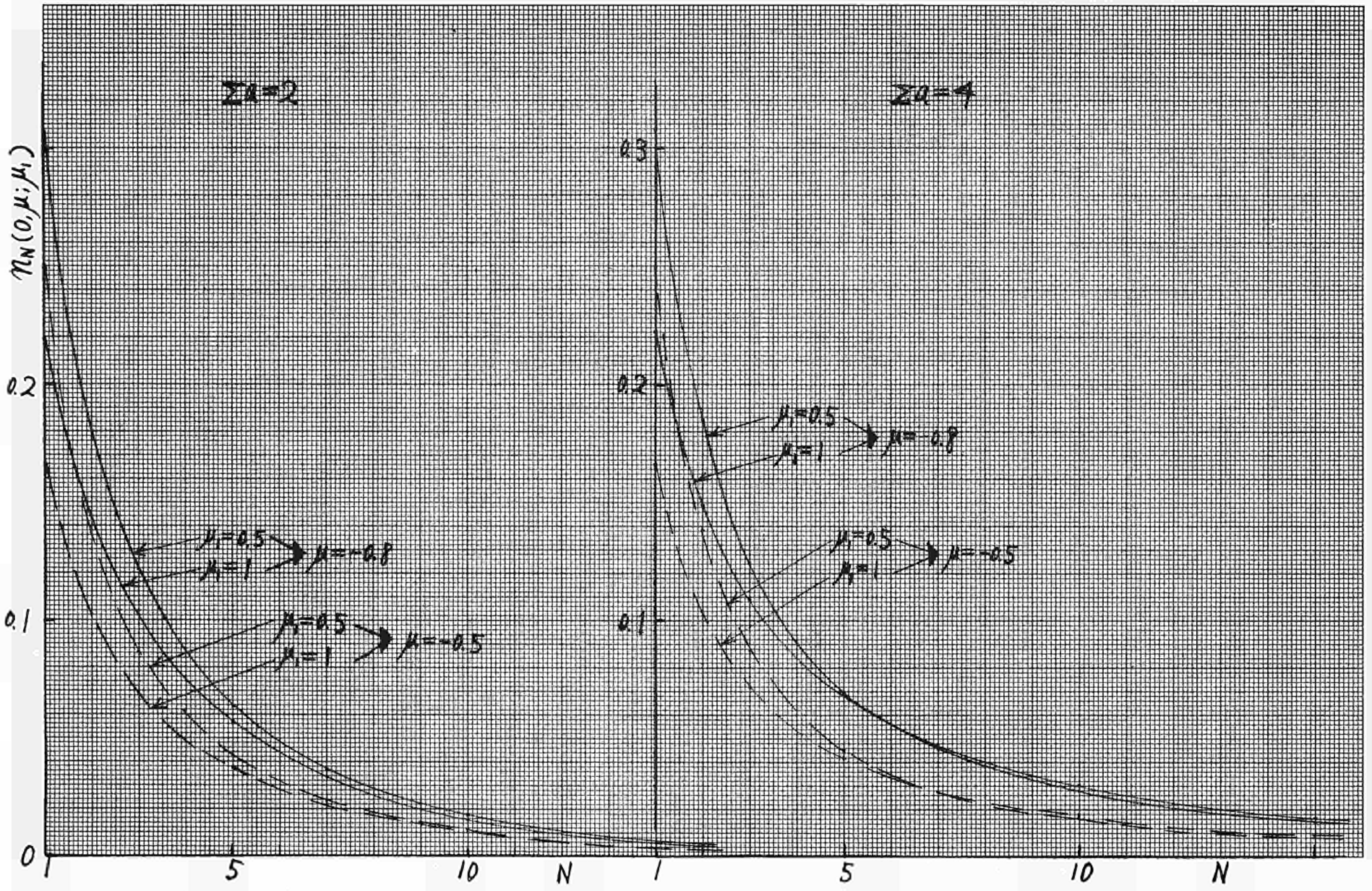

Fig. 14 – Number of neutrons transmitting after the first collision (monodirectional source)

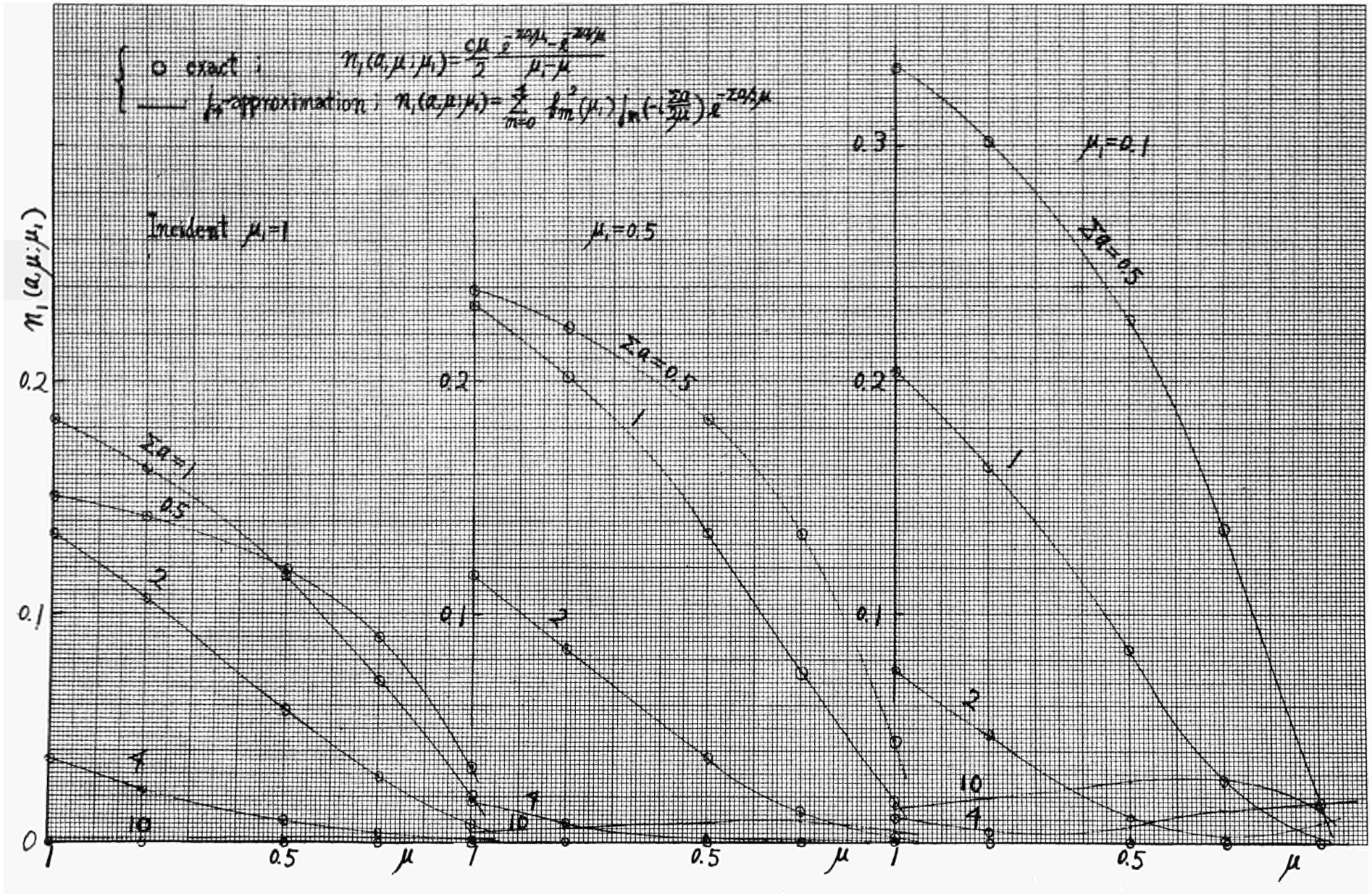

Fig. 15 – Number of neutrons transmitting after the second collision (monodirectional source)

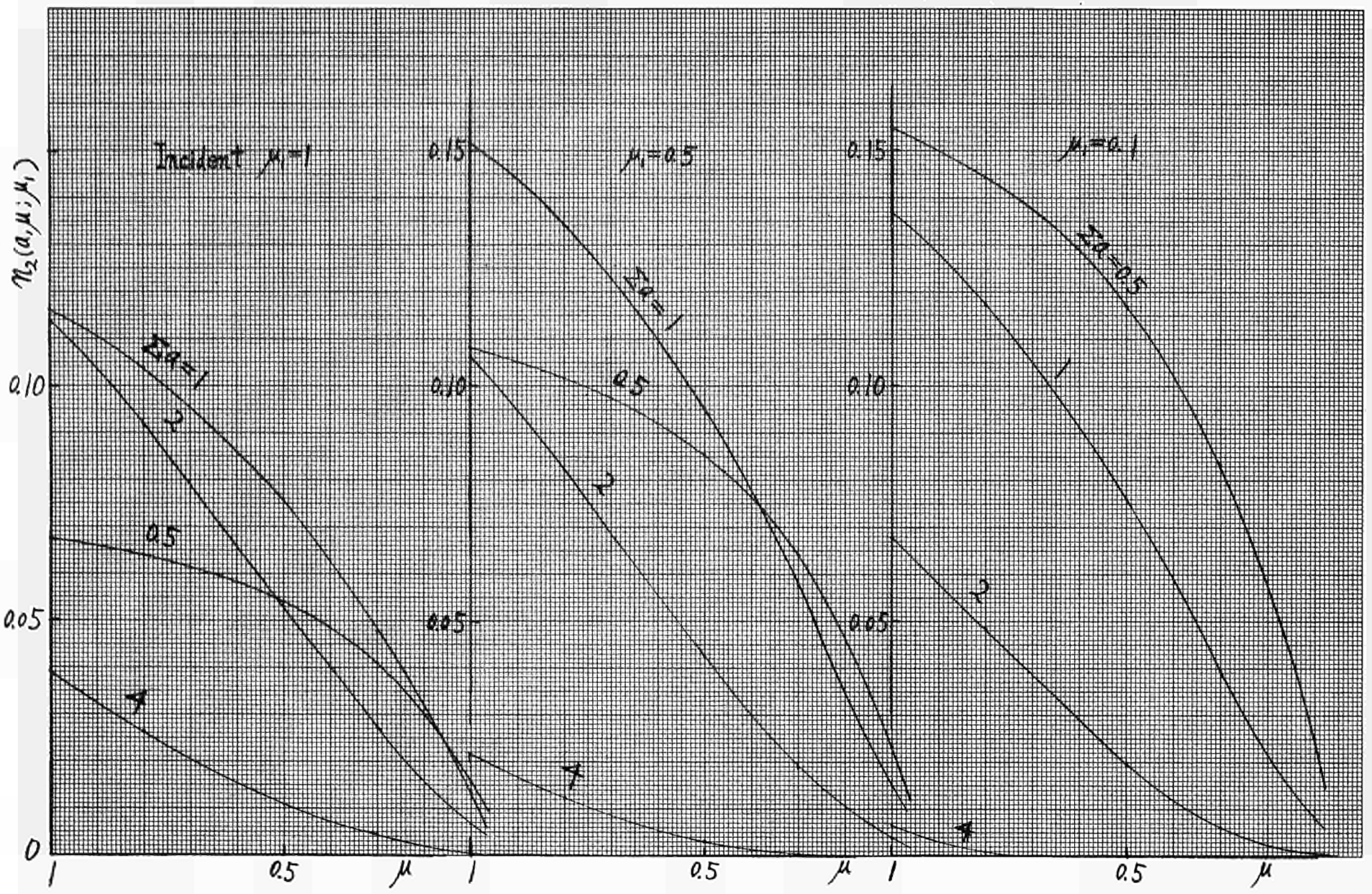

Fig. 16 – Number of neutrons transmitting after the third collision (monodirectional source)

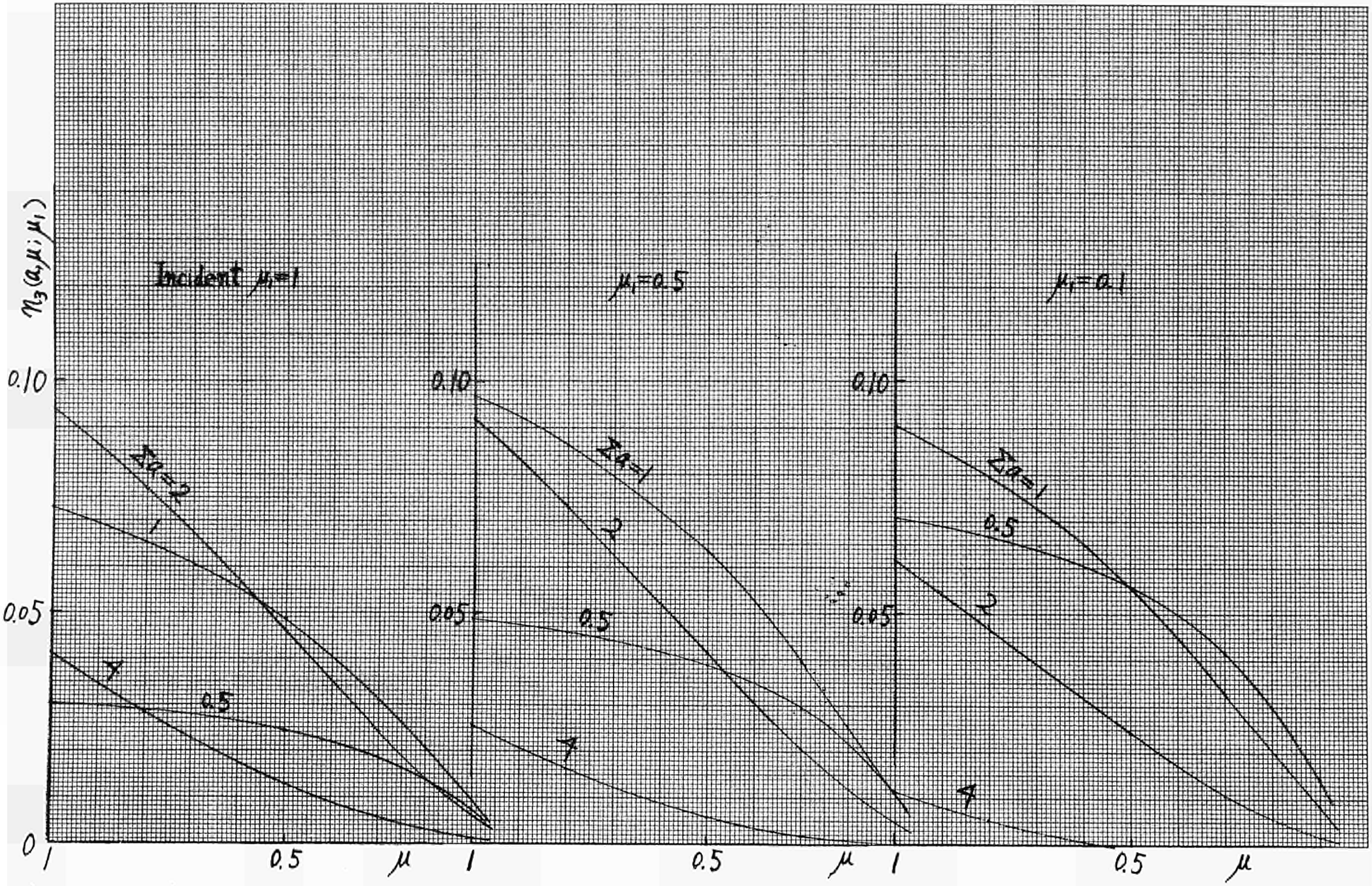

Fig. 17 — Number of neutrons transmitting after the 5-th collision (monodirectional source)

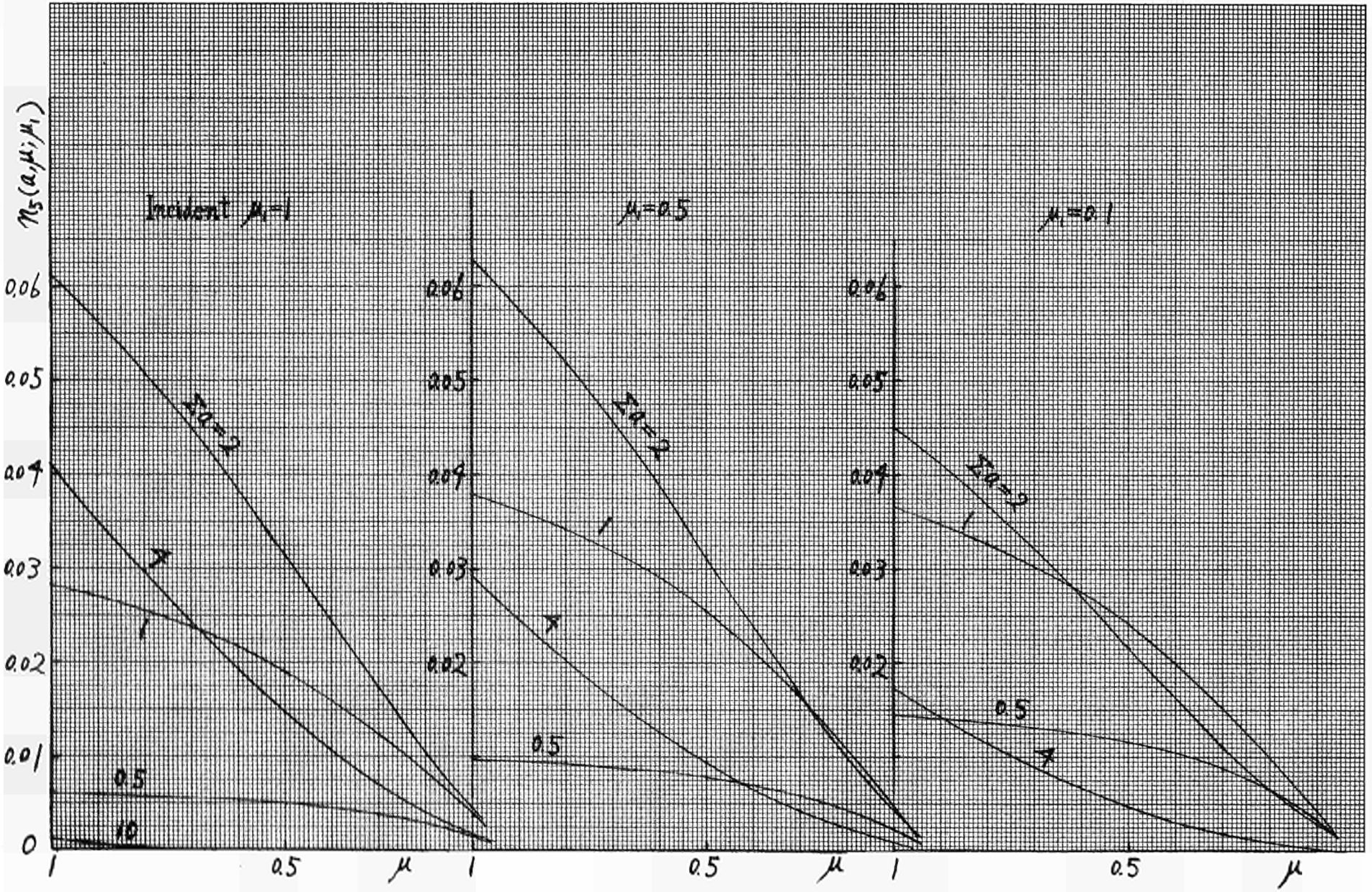

Fig. 18— Number of neutrons transmitting after the 7-th collision (monodirectional source)

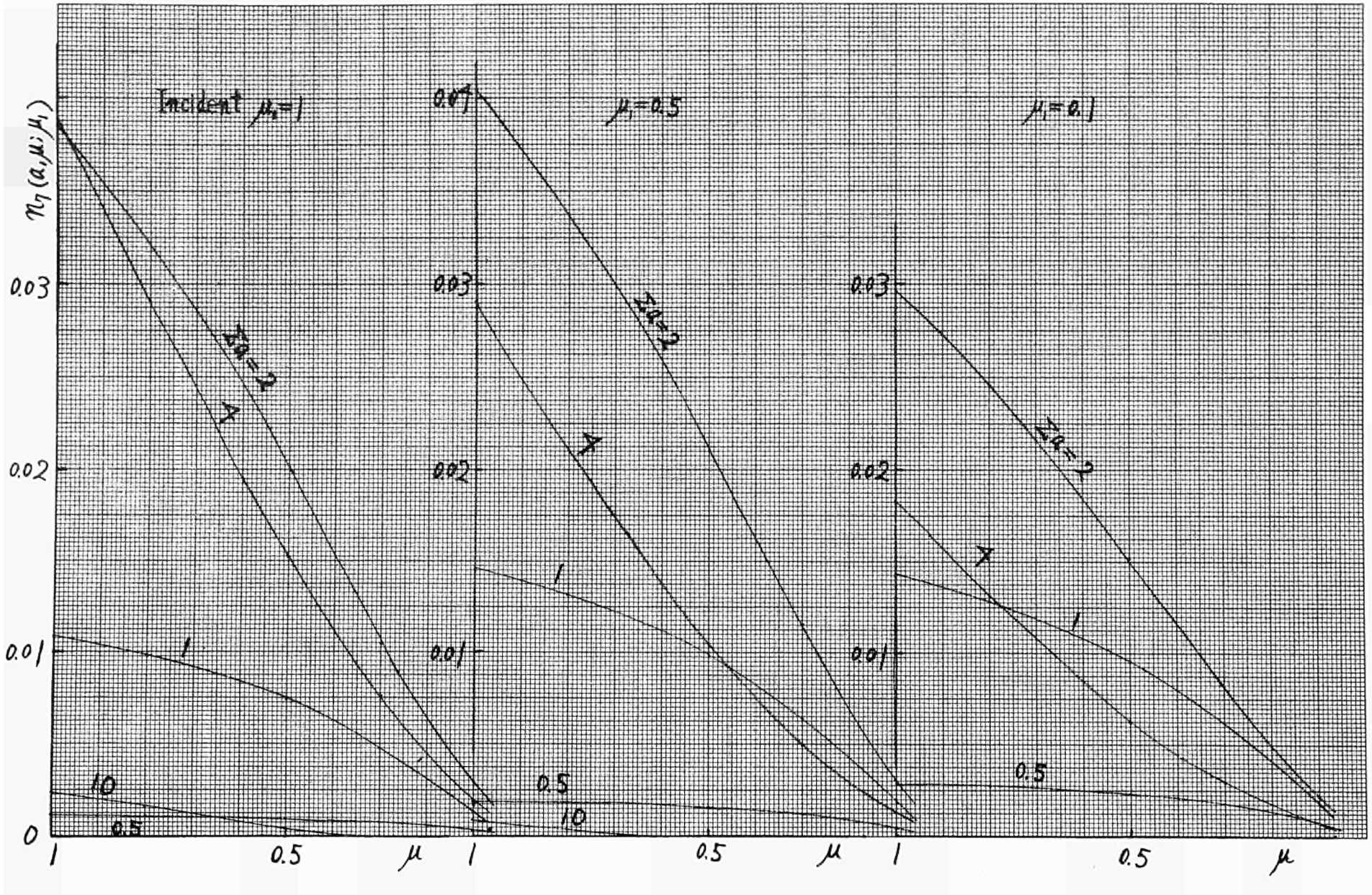

Fig. 19- Number of neutrons transmitting after the 10-th collision (monodirectional source)

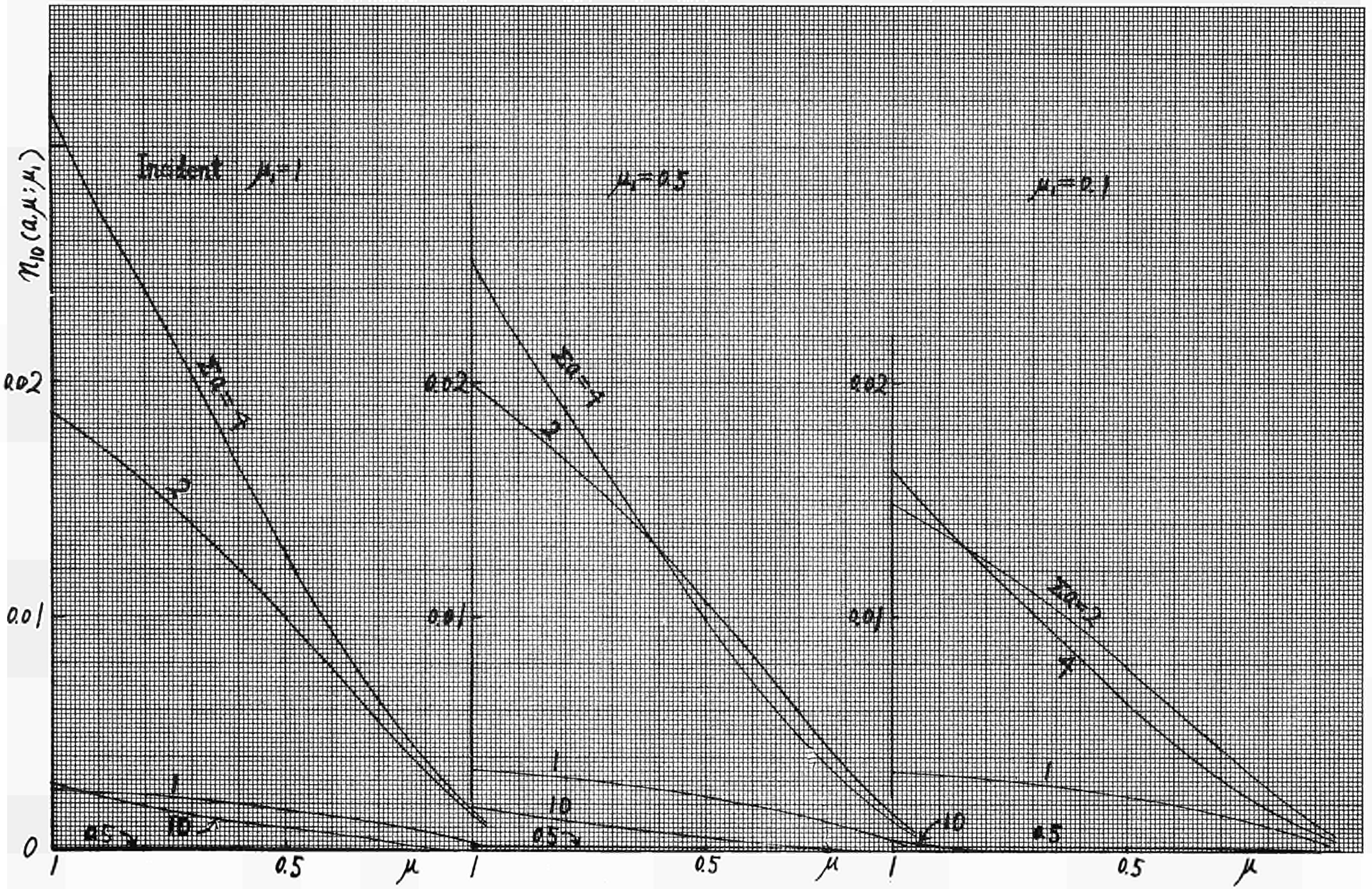

Fig. 20 – Number of neutrons transmitting after the 15-th collision (monodirectional source)

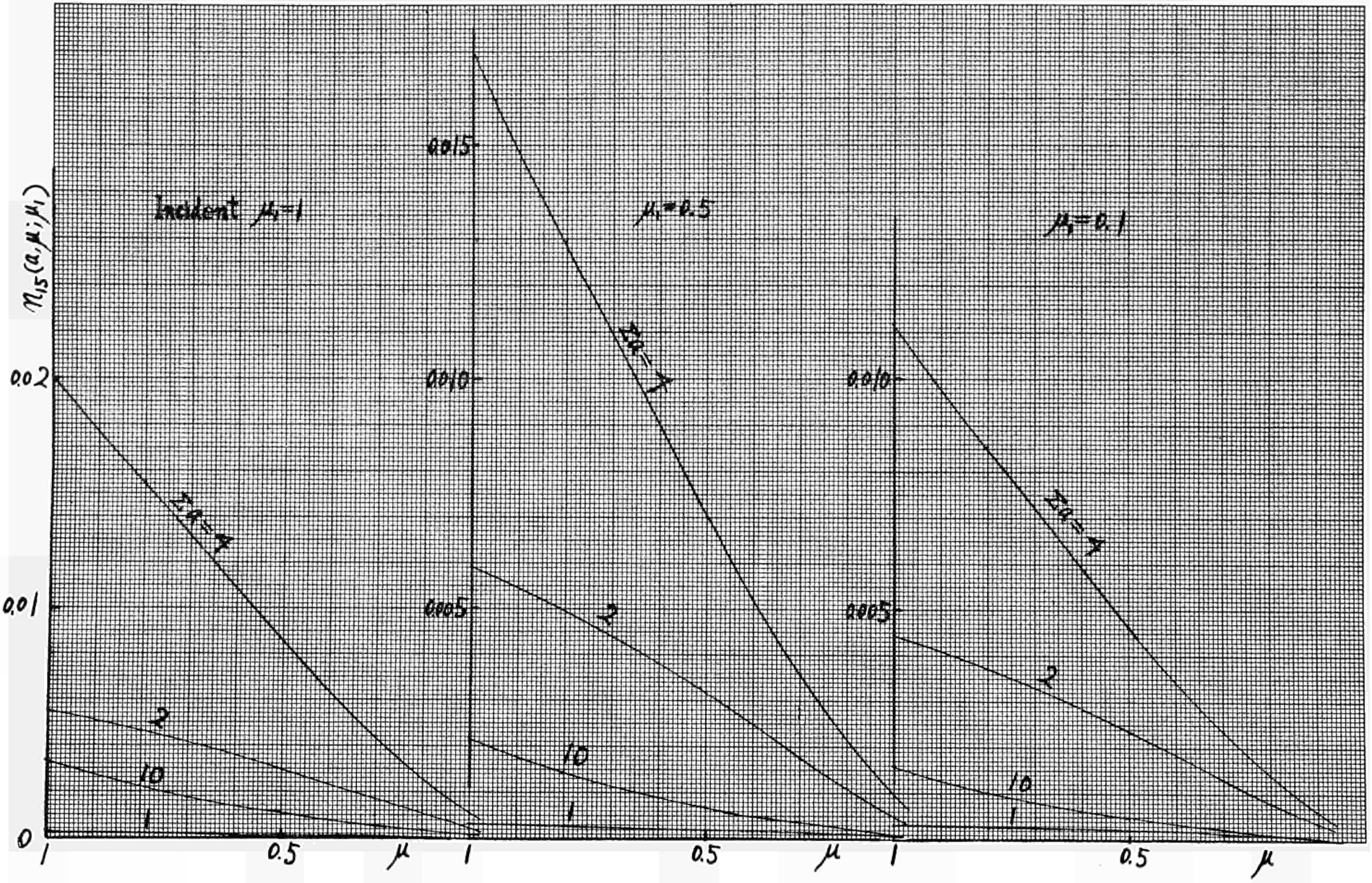

Fig. 21 — Number of neutrons transmitting after the 20-th collision (monodirectional source)

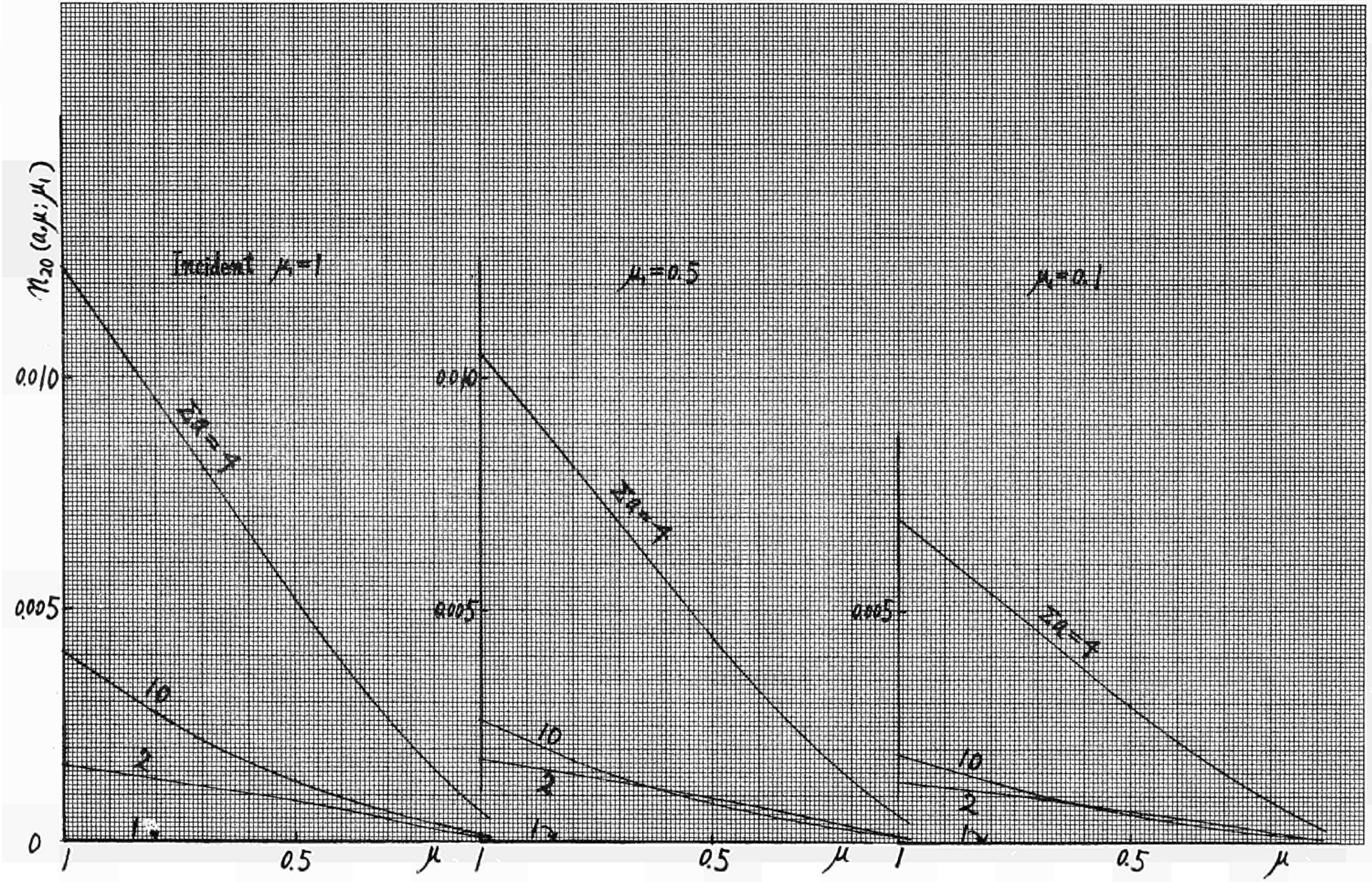

Fig. 22 — Number of neutrons transmitting after the 30-th collision (monodirectional source)

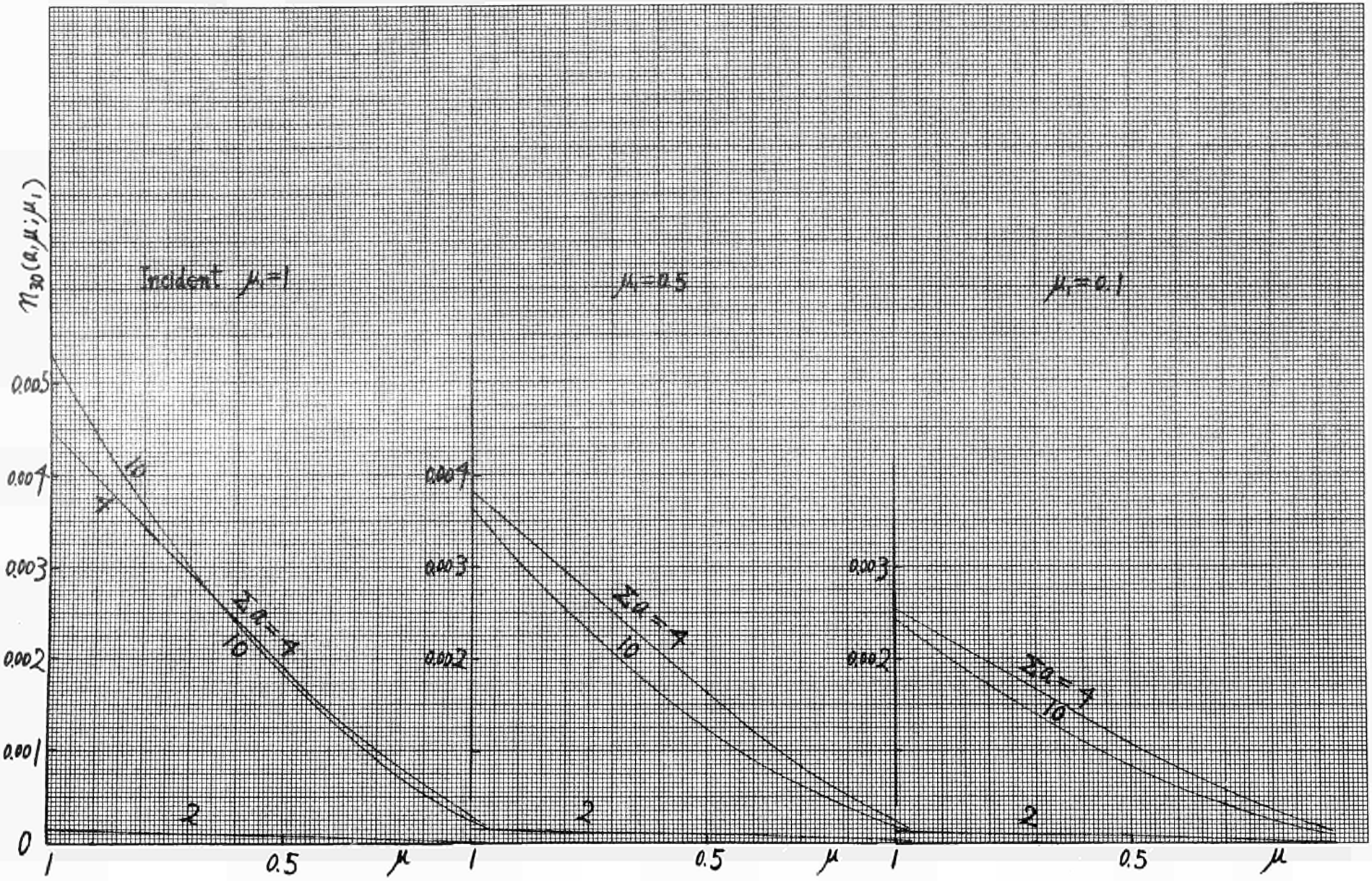

Fig. 23 – Number of neutrons transmitting after the 50-th or the 70-th collision (monodirectional source)

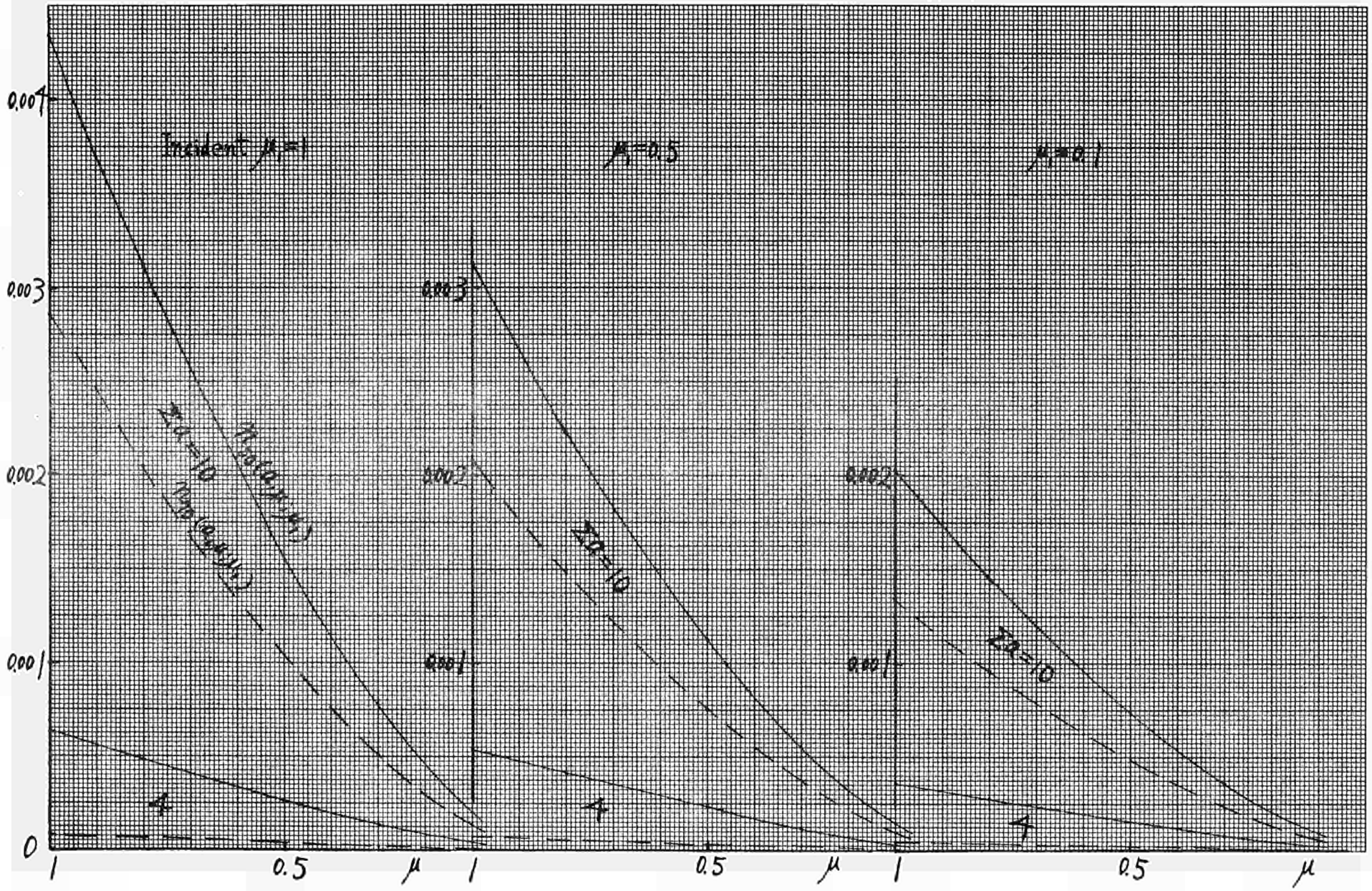

Fig. 24 – Number of neutrons transmitting the slab with $\Sigma a=2$ or 4 after the N-th collision (monodirectional source)

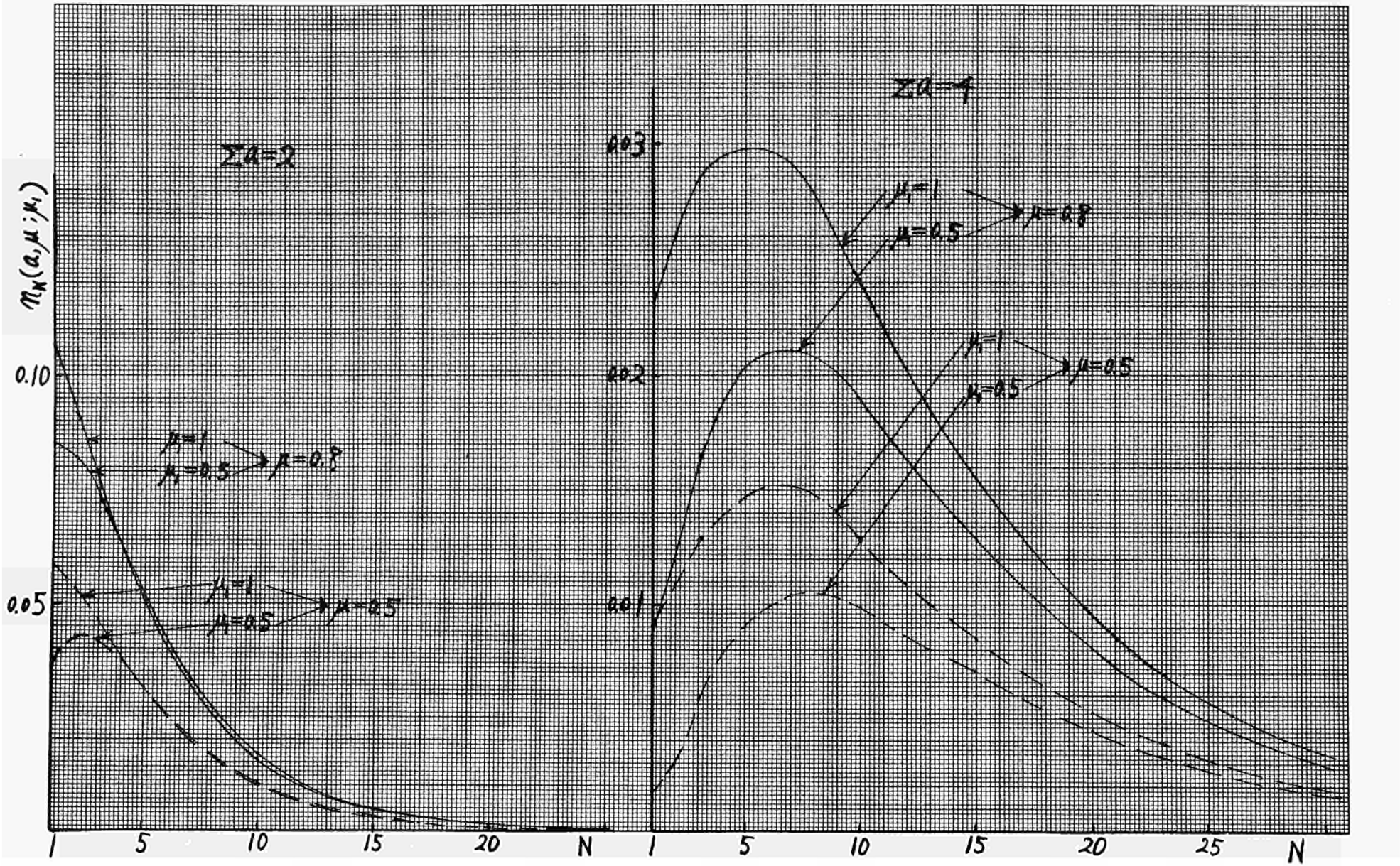

Fig. 25 — Total number of neutrons reflected by the slab (monodirectional source)

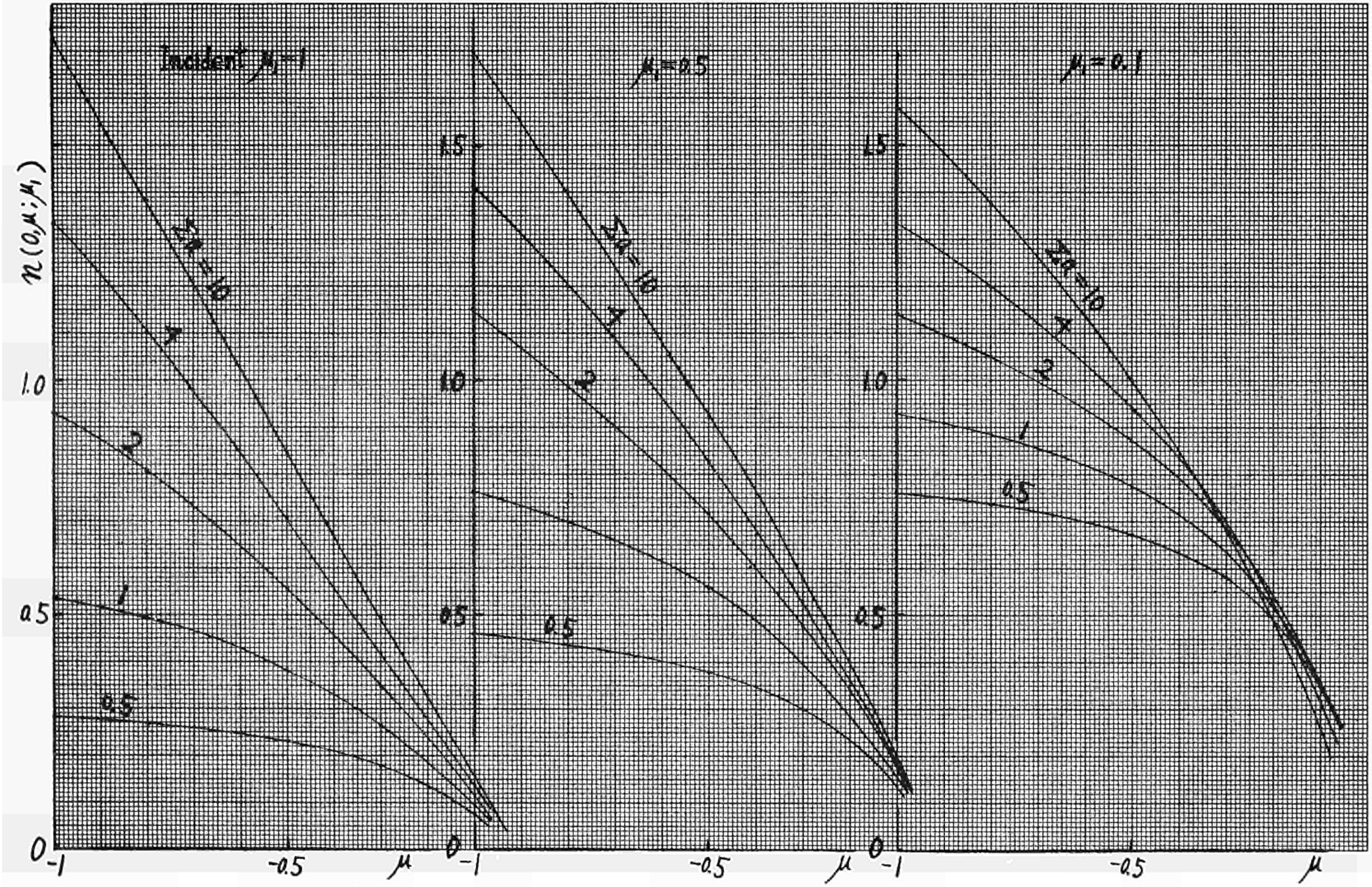

Fig. 26 — Total number of neutrons transmitting the slab (monodirectional source)

(The neutrons transmitting without collision are excluded; $\sum_{n=0}^{\infty} n_N(a,\mu;\mu_1) = n(a,\mu;\mu_1) - \delta(\mu-\mu_1)e^{-\Sigma a/\mu_1}$.)

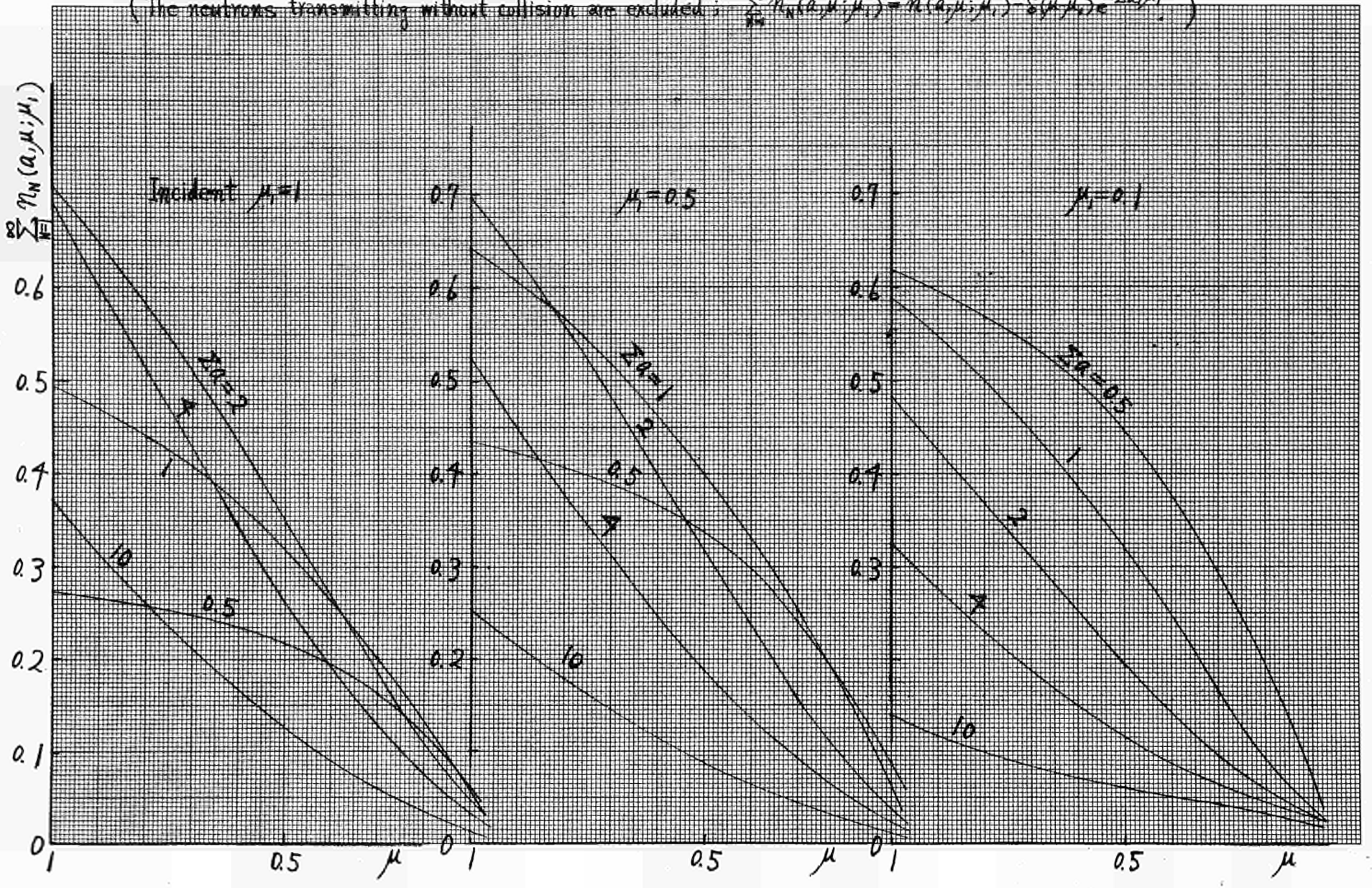

Fig. 27 – Number of neutrons reflected after the first, second or 5-th collision (isotropic source)

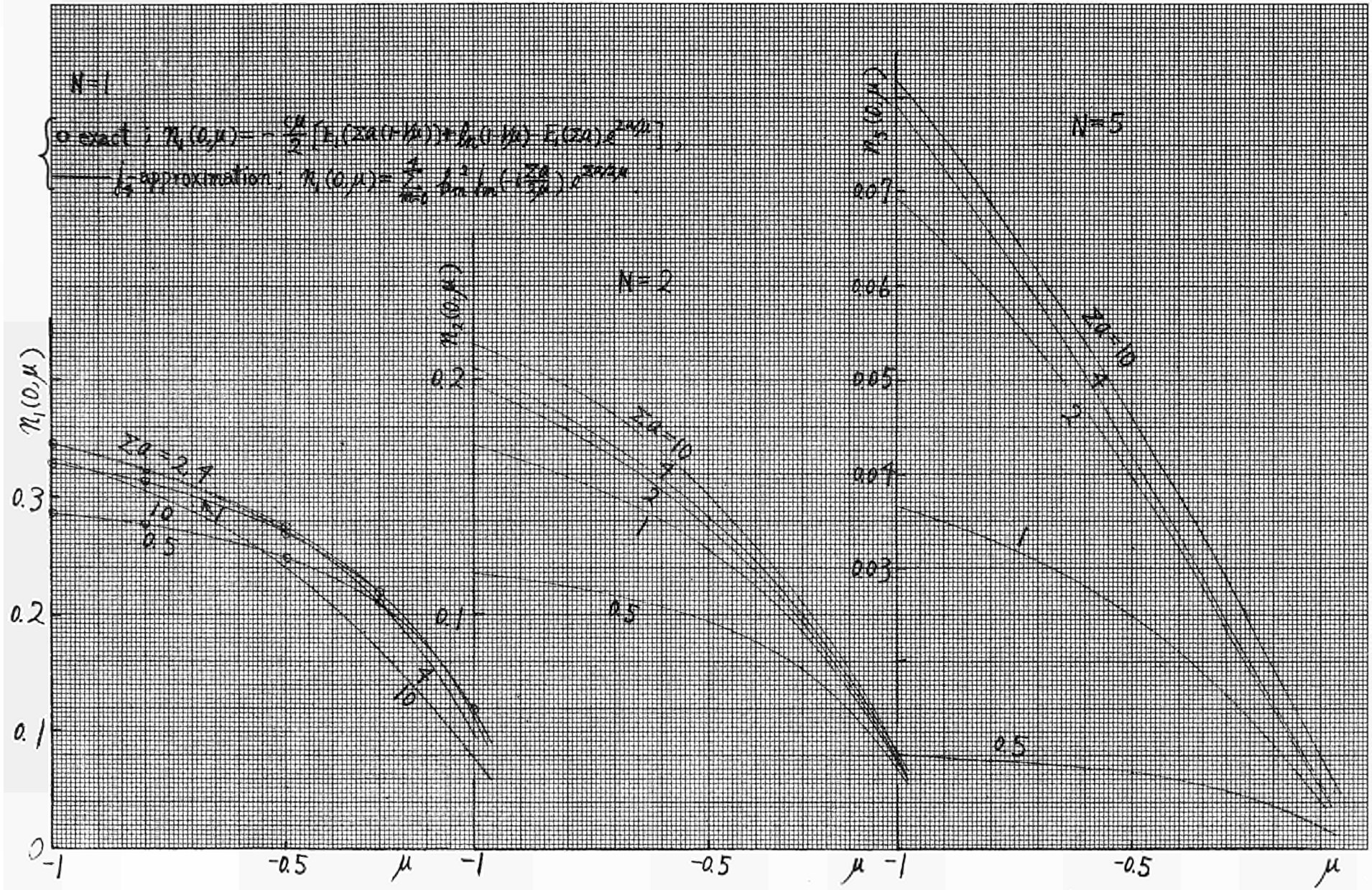

Fig. 28 – Number of neutrons reflected after the 10-th, 20-th, 30-th, 50-th, 70-th or 100-th collision (isotropic source)

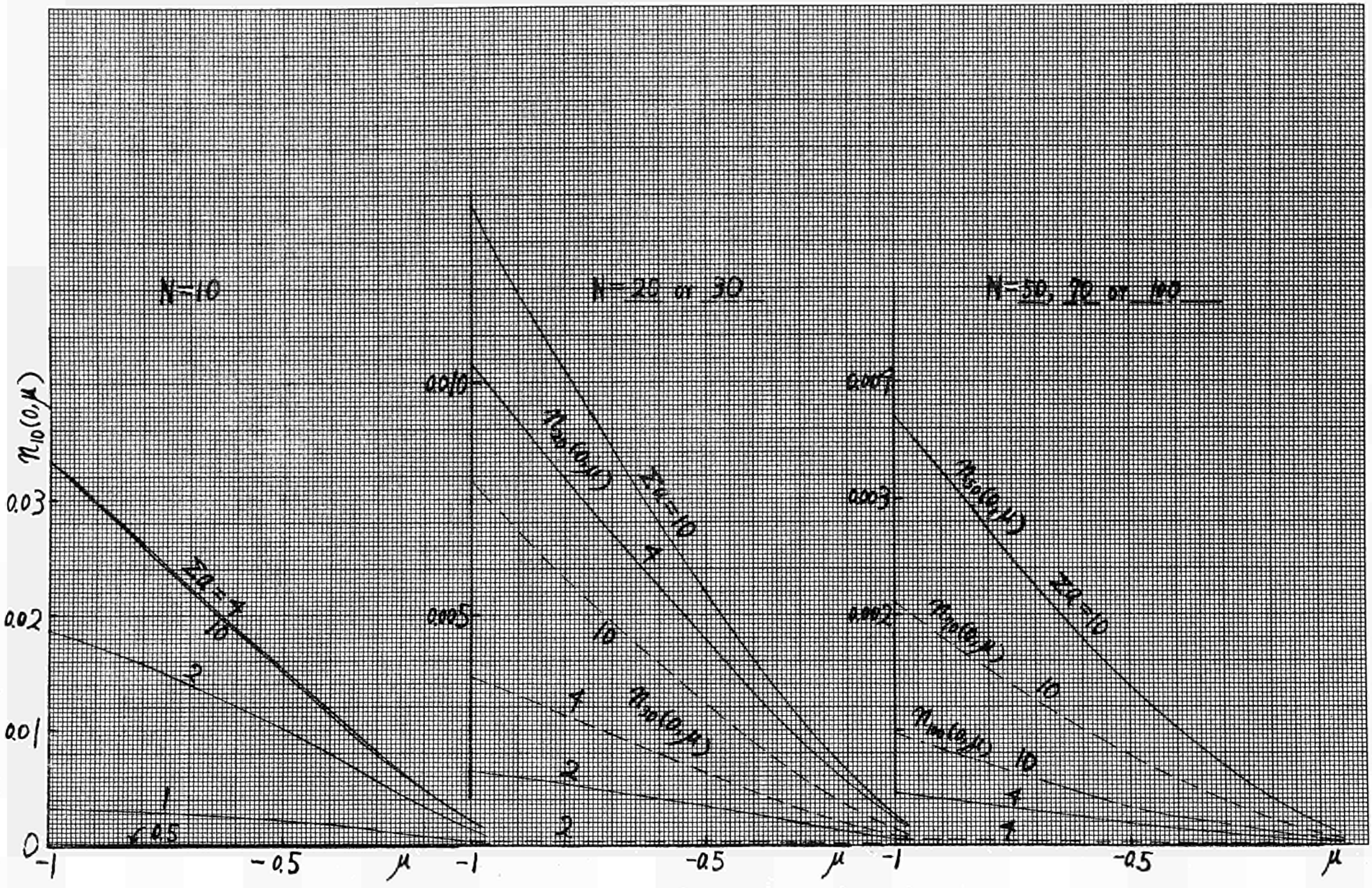

Fig. 29 – Number of neutrons transmitting after the first, second or 5-th collision (isotropic source)

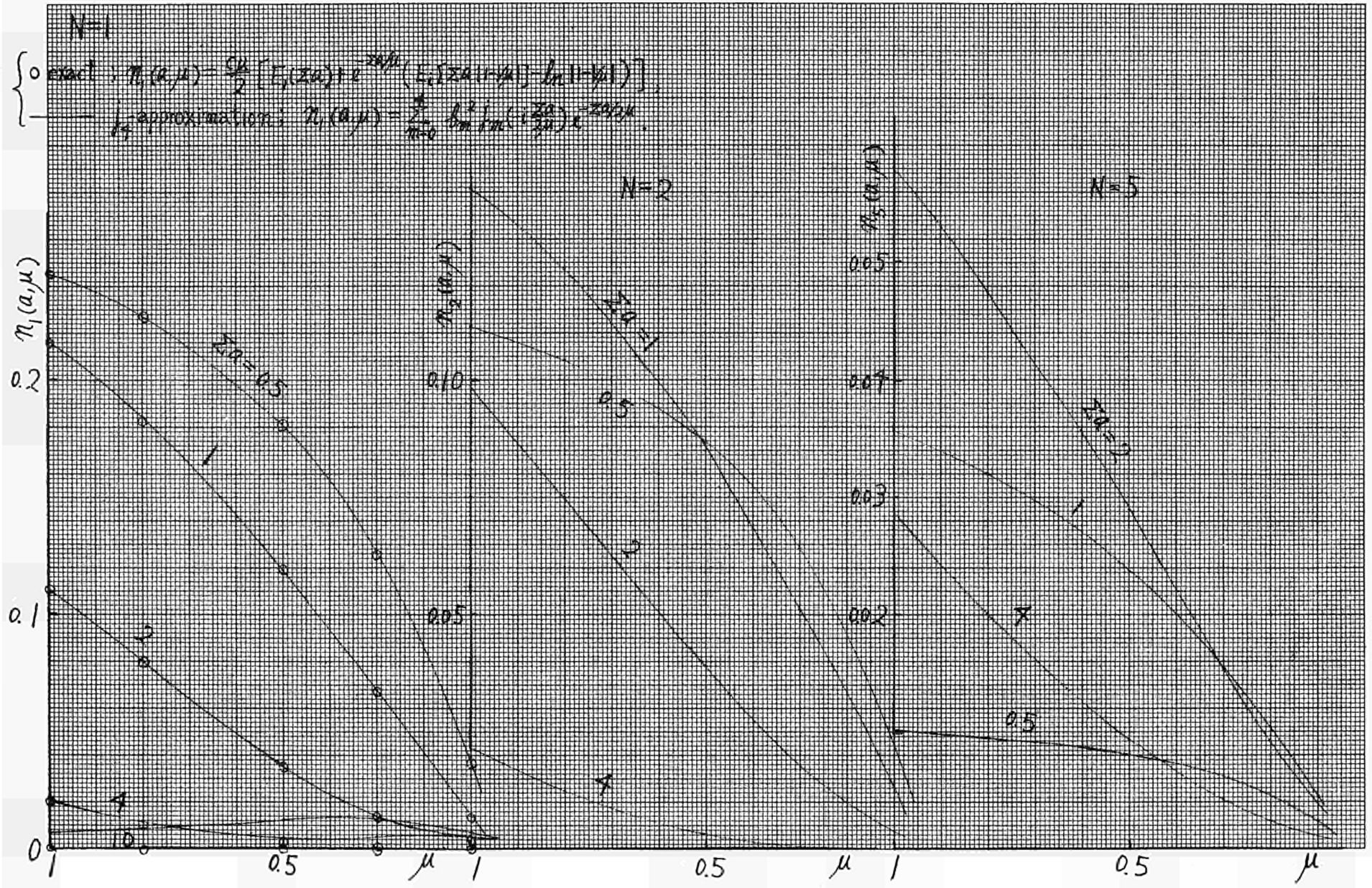

Fig. 30 – Number of neutrons transmitting after the 10-th, 20-th, 30-th, 50-th, 70-th or 100-th collision (isotropic source)

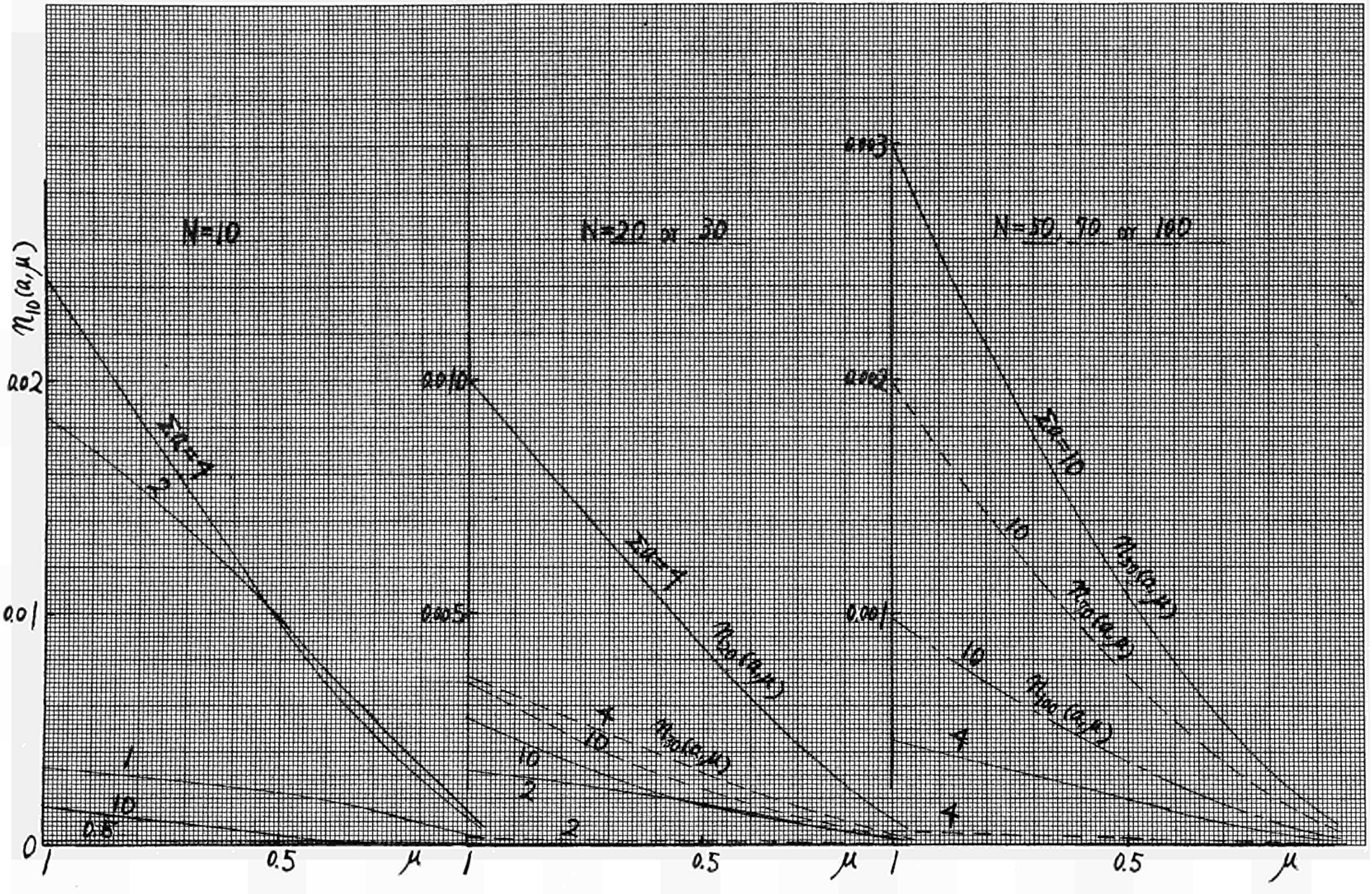

Fig. 31 – Total number of neutrons reflected by or transmitting the slab (isotropic source)